The use of semianalytic confidence limit calculations in searches for new particles at LEP200

Morten Schiøtz

August 30, 1999

Thesis submitted to the Cand. Scient. Degree
Department of physics
University of Oslo

Abstract

In this thesis a description of a semi analytic method of confidence limit calculations in searches with several distinct channels is given. A comparison between different implementations show that, in a search with many channels, a histogram type implementation is both faster and more accurate than a list, or vector, type implementation, when compared to a Monte Carlo routine. However, in the 1998 DELPHI search for the neutral Higgs boson, both the list type and the histogram type implementations yields within 50 MeV the same limit on the Higgs boson mass as the Monte Carlo routine, which gives a lower limit of 85.7 GeV at a 95 % confidence limit. In searches with few channels the list type implementation is as fast and accurate as the histogram type.

In a search for W decaying into a chargino-neutralino pair, which is an example of a search with few channels, data collected at DELPHI during the $\sqrt{s}$=183 GeV run of 1997 and the $\sqrt{s}$=172 GeV of 1996 have been analyzed. The branching ratio was calculated to be $BR(W^{\pm} \rightarrow \tilde{\chi}_1^{\pm}\tilde{\chi}_1^0)$ <1.34% at 95 % confidence limit.

Preface

I would like to thank my supervisor, Alex Read, for giving me the opportunity to work with these interesting problems, and his help throughout this thesis. I would also like to give Ph.D student Trond Myklebust a special thanks, for always fixing the computers whenever they broke down. A warm thank-you also goes to the other students at the High Energy Physics group, for being so fun to work with.

Oslo, 30 august 1999
Morten Schiøtz

Contents

Chapter 1

Introduction

In the fifties, common belief was that the proton, the neutron and the electron were the elementary particles, *i.e.* that out of these three particles all other particles was built. However, during this period a bunch of new particles was discovered, which culliminated with the quark theory of Zweig and Gell-Mann. The fundamental particles are now believed to be the fermions, which are the matter particles, and the bosons, which acts as force carriers between the fermions, see Fig. 1.1.

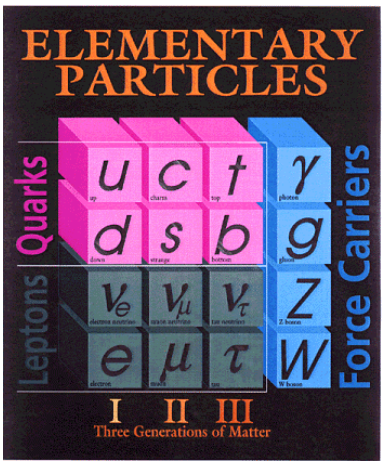

Figure 1.1: The different particles of the Standard Model. The fermions, *i.e.* matter particles, are divided into three different generations, or families, and interacts by exchange of the bosons.

The Standard Model is briefly described in Chapter 2. Although the Standard Model is the most successful theory in the history of physics, at least when it comes to experimental predictability, it has some serious theoretical shortcomings. The masses of the different fundamental particles

and several mixing angles are arbitrary parameters, which adds up to over 20. This high number of free parameters is not popular with physicists. As an attempt to theoretically fix the masses, the Higgs mechanism is introduced. If this is the way nature works, a new particle, the Higgs boson, is also introduced with the Higgs mechanism. So far this particle has not been detected experimentally. A theoretical flaw of the Standard Model is that self-interactions of the Higgs boson gives it a mass of infinity, which is not good. Enter supersymmetry. In supersymmetric theories, all particles have supersymmetric partners, where the spin is shifted by one-half. This means that the self-interactions of the Higgs boson consists of equal parts of fermionic and bosonic self interactions. These terms enter the calculations with opposite signs, giving the Higgs boson a physical mass. Unfortunately, this symmetry of particles and supersymmetric partners cannot be an exact symmetry, since no experiment has ever detected a supersymmetric particle.

In order to test these theories, large experiments around the world have been made. Typical particle physics experiments collides different particles with high energy in some manner. Most standard experiments are either linear or circular accelerators. The linear accelerator accelerates particles in a straight vacuum tube, and collides the particles with a fixed target. The circular accelerates particles of one kind in one direction in a circular vacuum tube, and particles of another type in the opposite direction, and collides these beams of particles at certain places around the tube where detectors are placed. Due to Einstein's relation of mass and energy, $E = mc^2$, the large energy of the particles being collided is transformed into heavier and hopefully new particles. In Chapter 3 the detector responsible for the data discussed in this thesis, the DELPHI detector, which is one of the experiments at CERNs Large Electron Positron collider, is described.

When the data has been collected, one has, in one way or another to compare the experimental data with the theoretical model being tested, in order to see if something new has been observed. This can be done by calculating which Standard Model processes one would expect in the experiment, and then see how the data compare to this expected background. This statistical treatment of data will be discussed in Chapter 4.

Searches for the two scenarios described above, the Standard Model and the Minimal Supersymmetric extension of the Standard Model, and the statistical treatment of the data produced by two searches are described in Chapters 5 and 7. An essential part of the discussion is my semianalytical confidence limit calculator `SA_COUNTING`, which has taken lots of blood, sweat and tears to understand and implement. This interpretation of the statistical method described in Chapter 3 has been compared to two other interpretations of the same method and a Monte Carlo method in Chapter 4.

`SUSYPAR`, see Appendix B, which also has been implemented at the cost of some sleepless nights, has been used to perform the parameter exclusion

in a special parameter space in the Minimal Supersymmetric extension of the Standard Model. Although MSSM is not plagued by the large numbers of free parameters as the Standard Model is, there are still a few mass parameters and mixing angles left to experiment to be determined. Since there is no experimental evidence of sypersymmetry so far, only some sort of exclusion is possible.

Chapter 2

Particle Physics Theory

2.1 The Standard Model

The interactions between the known elementary particles, the *fermions*, matter particles, and the *bosons*, force carriers, are described in the Standard Model of particle physics (SM). The interactions can be divided into three different types of forces: the strong, the electromagnetic and the weak forces. In some theories, Grand Unified Theories (GUT), these three forces are united at a very large scale, 10^{16} GeV, see Fig. 2.1. However, at present energies these forces remain separate.

The inspiration of this section is mostly found in *"Dynamics of the Standard Model"* [1]. The different interactions are described by Lagrangians with local gauge invariance.

2.1.1 The interactions

Quantum Electrodynamics (QED)

In QED the electromagnetic interactions between fermions and photons are described. This is the part of the Standard Model that has been verified most thoroughly by experiments.

Under a local $U(1)$ QED gauge transformation, $\psi \rightarrow e^{i\alpha(x)}\psi$, the Lagrangian

$$\mathcal{L} = i\bar{\psi}\gamma^{\mu}\partial_{\mu}\psi - m\bar{\psi}\psi \tag{2.1}$$

is not invariant. Under this gauge transformation, the adjoint wave equation transforms as $\psi \rightarrow e^{-i\alpha(x)}\bar{\psi}$. When inserting the transformed wave equations into the Lagrangian, it takes this form:

$$\mathcal{L} = ie^{-i\alpha(x)}\bar{\psi}\gamma^{\mu}\partial_{\mu}e^{i\alpha(x)}\psi - e^{-i\alpha(x)}e^{i\alpha(x)}m\bar{\psi}\psi \tag{2.2}$$

The first term is not invariant, since $\partial_{\mu}e^{i\alpha(x)}\psi = e^{i\alpha(x)}\partial_{\mu}\psi + ie^{i\alpha(x)}\psi\partial_{\mu}\alpha(x) \neq e^{i\alpha(x)}\partial_{\mu}\psi$. By exchanging ∂_{μ} with a "covariant derivative" operator D_{μ},

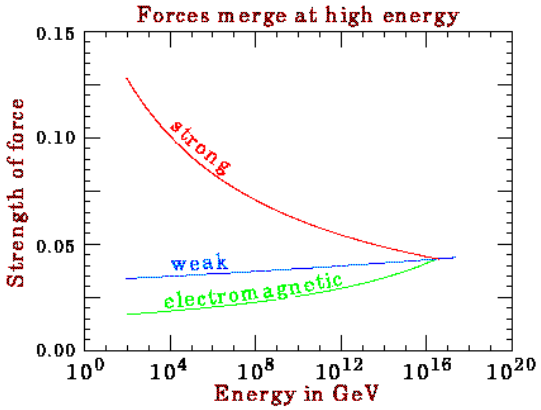

Figure 2.1: The development of the coupling constant, and where they will be united according to Grand Unified Theories.

which transforms as $D_\mu \rightarrow e^{i\alpha(x)} D_\mu \psi$, invariance of the Lagrangian can be ensured. One possible covariant derivative is:

$$\begin{aligned} D_\mu &\equiv \partial_\mu - ieA_\mu \\ A_\mu &\rightarrow A_\mu + \frac{1}{e}\partial_\mu \alpha. \end{aligned} \tag{2.3}$$

With this operator, the Lagrangian takes the form

$$\begin{aligned} \mathcal{L}_{QED} &= i\bar{\psi}\gamma^\mu D_\mu \psi - m\bar{\psi}\psi \\ \mathcal{L}_{QED} &= \bar{\psi}(i\gamma^\mu \partial_\mu - m)\psi + e\bar{\psi}\gamma^\mu A_\mu \psi - \frac{1}{4}F_{\mu\nu}F^{\mu\nu}. \end{aligned} \tag{2.4}$$

The last term includes the invariant field strength tensor $F_{\mu\nu}$ to ensure invariance of the kinematic term. Since there is no $-m^2 A_\mu A^\mu$ term in the QED Lagrangian, the QED gauge particle, which is the photon A_μ, is massless.

Quantum Chromodynamics (QCD)

The QCD Lagrangian, describing the interactions between massive quarks and massless gluons, is more complex than its QED partner, since the gluons carry color charge. There are eight different gluons, each carrying one of three colors, and can thus interact with each other. The QED Lagrangian just needs to take one type of photon, which is charge neutral into consideration (color charge has nothing to do with electrical charge though).

Weak interactions. The Weinberg-Salam model.

Most hadrons experience the weak force and can decay through weak interactions, but since QED and QCD decays are much faster than the weak

decays, they tend to dominate. Particles which decay through strong interactions have a lifetime in the order 10^{-23} seconds, particles which decays through electromagnetic interactions have lifetimes in the order of 10^{-16} seconds and particles decaying through weak interactions have lifetimes in the order of 10^{-8} seconds. Some processes that are forbidden in electromagnetic or strong interactions, such as decays of the π meson, may decay through the weak force. Often weak processes include the creation of neutrinos, which interacts only through the weak forces, but this is not a requirement.

The main quantum numbers in the weak theory are the weak hypercharge, Y_w, and the weak isospin, T_i defined by the linear relation $Q = T_3 + \frac{Y}{2}$ where Q is the electrical charge.

The gauge fields that couples to the weak quantum numbers are the $\vec{W}^i_\mu$, with $i = 1,2,3$, which couples to the weak isospin and B_μ to the weak hypercharge. These fields give rise to the pure-gauge part of the weak Lagrangian

$$\mathcal{L}_{Gauge} = -\frac{1}{4}F^{\mu\nu}_i F^i_{\mu\nu} - \frac{1}{4}B^{\mu\nu}B_{\mu\nu}, \tag{2.5}$$

with $F^i_{\mu\nu}$ and $B_{\mu\nu}$ as the $SU(2)_L$ and $U(1)_Y$ field strength. The L subscript of $SU(2)_L$ is a reminder that since the neutrinos are (nearly) massless, they only have left handed components. The $SU(2)_L$ covariant derivative,

$$D_\mu = \left((\partial_\mu + i\frac{g_1}{2}Y_w B_\mu) + ig_2\frac{\vec{\tau}}{2}\vec{W}_\mu \right) \tag{2.6}$$

where g_1 and g_2 are, respectively, the $U(1)_Y$ and $SU(2)_L$ gauge coupling constants, ensures invariance of the Lagrangian, but with this pair of Lagrangian and covariant derivative the fermions and gauge bosons are massless particles. The massless gauge bosons born when the gauge symmetry is broken are named Goldstone bosons. By introducing a complex doublet, the Higgs field

$$\Phi = \begin{pmatrix} \phi^+ \\ \phi^0 \end{pmatrix}, \tag{2.7}$$

the full weak Lagrangian with masses for the physical particles can be found by adding the Lagrangians for the Higgs-fermion and Higgs-boson couplings to the pure-gauge Lagrangian. The Higgs-fermion Lagrangian, $\mathcal{L}_{Hf}$, and Higgs-boson Lagrangian, $\mathcal{L}_{Hb}$, are given by

$$\mathcal{L}_{Hf} = -f_u\bar{q}_L\tilde{\Phi}u_R - f_d\bar{q}_L\Phi d_R - f_e\bar{l}\Phi e_R + h.c. \tag{2.8}$$

$$\mathcal{L}_{Hb} = (D^\mu\Phi)^* D_\mu\Phi - (-\mu^2\Phi^\dagger\Phi + \lambda(\Phi^\dagger\Phi)^2) \tag{2.9}$$

where $\tilde{\Phi}$ is the charge conjugate of the Higgs field, $\tilde{\Phi} = i\tau_2\Phi^*$, f_i are constants which must be determined by experiment and D_μ is the appropriate

covariant derivative,

$$D_\mu = \left((\partial_\mu + i\frac{g_1}{2}B_\mu) + ig_2\frac{\vec{\tau}}{2}\vec{W}_\mu \right), \tag{2.10}$$

where $\vec{\tau}$ are the Pauli matrices. The Higgs-fermion Lagrangian shown here includes only the first generation of fermions for simplicity.

The masses of the different particles are found by performing a spontaneous symmetry breaking of the Higgs self interactions,

$$\frac{\partial V}{\partial \Phi} = \frac{\partial}{\partial \Phi}\left(-\mu^2\Phi^\dagger\Phi + \lambda(\Phi^\dagger\Phi)^2\right) = \Phi(-\mu^2 + \lambda\Phi^2) = 0. \tag{2.11}$$

Perturbations around the non-trivial minimum of the Higgs potential breaks the symmetry of the Lagrangian spontaneously. By inserting the vacuum state describing this system,

$$\langle\Phi\rangle_0 = \begin{pmatrix} 0 \\ v/\sqrt{2} \end{pmatrix}, \tag{2.12}$$

where $v \equiv \sqrt{\mu^2/\lambda} = 1/\sqrt{\sqrt{2}G}$ has been found by experiments to be 246 GeV, into the Higgs Lagrangian, the mass terms are found,

$$\begin{aligned} \mathcal{L}_{mass} \;=\; & -\tfrac{v}{\sqrt{2}}(f_u\bar{u}u + f_d\bar{d}d + f_e\bar{e}e) + \left(\tfrac{vg_2}{2}\right)^2 W_\mu^+ W_-^\mu \\ & +\tfrac{v^2}{8}(W_\mu^3 B_\mu)\begin{pmatrix} g_2^2 & -g_1g_2 \\ -g_1g_2 & g_1^2 \end{pmatrix}\begin{pmatrix} W_\mu^3 \\ B_\mu \end{pmatrix} \end{aligned} \tag{2.13}$$

giving the fermions and bosons masses. The Higgs mass, which can be found to be $m_H^2 = \frac{\partial V^2}{\partial^2\Phi}|_{\Phi=v} = \lambda v^2/\sqrt{2}$, remains unknown, since of the free parameters μ and λ only their ratio v is known. The first term of Eq. 2.13 gives the fermion masses:

$$m_i = \frac{v}{2}f_i, \tag{2.14}$$

The second term of Eq. 2.13 gives the masses of the charged gauge bosons, $m_W = \frac{v}{2}g_2$. Introduction of spontaneous symmetry breaking mix the neutral fields, seen in the mass third term of the Lagrangian. Defining the weak mixing angle as the ratio of the gauge couplings

$$\tan\theta_W \equiv \frac{g_1}{g_2}, \tag{2.15}$$

one can define the basis

$$A_\mu = \cos\theta_W W_\mu^3 - \sin\theta_W B_\mu \tag{2.16}$$

$$Z_\mu = \sin\theta_W W_\mu^3 + \cos\theta_W B_\mu. \tag{2.17}$$

particle		spin	sparticle		spin
quark	q	1/2	squark	$\tilde{q}_{L,R}$	0
charged lepton	l	1/2	charged slepton	$\tilde{f}$	0
neutrino	ν	1/2	sneutrino	$\tilde{l}_{L,R}$	0
gluon	g	1	gluino	$\tilde{g}$	1/2
photon	γ	1	photino	$\tilde{\gamma}$	1/2
	Z_0	1	zino	$\tilde{Z}$	1/2
	$W^{\pm}$	1	wino	$\tilde{W}^{\pm}$	1/2
neutral Higgses	h, H, A	0	neutral Higgsinos	$\tilde{H}^0_{1,2}$	1/2
charged Higgses	$H^{\pm}$	0	charged Higgsinos	$\tilde{H}^{\pm}$	1/2
graviton	G	2	gravitino	$\tilde{G}$	3/2

Table 2.1: The SM particle and their MSSM sparticle partners

which diagonalize the third term of Eq. 2.13, which is the neutral gauge mass matrix. The physical particles corresponding to the neutral fields A_μ and Z_μ are the massless photon and the massive Z^0 boson. Their masses are $m_\gamma = 0$ and $M_Z = \sqrt{g_1^2 + g_2^2}$. The ratio of the charged and the neutral gauge particles are fixed by the weak mixing angle

$$\frac{M_W}{M_Z} = \cos\theta_W . \tag{2.18}$$

2.2 Going beyond the Standard Model

Most of the contents in this section is inspired by the SUSYGEN [4] manual and *"The Higgs Hunter's Guide"* [2].

A major problem arises when generating masses with the Higgs mechanism in the Standard Model. When trying to find the Higgs mass at higher order, loop diagrams like the one found in Fig. 2.2 adds up to give a Higgs mass of infinity. This is known as the hierarchy problem. To avoid this prob-

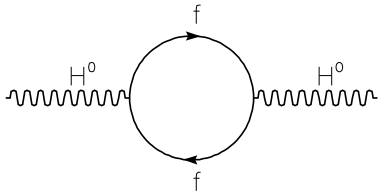

Figure 2.2: One-loop contribution to the Higgs mass. It is loop diagrams such as this that give rise to the hierarchy problem.

lem, supersymmetric theories (SUSY) introduce supersymmetric partners,

see Table 2.1, to all elementary particles. The fermions gets bosonic superpartners and the bosons gets fermionic spartners. These sparticles have their spin shifted by one-half compared to their SM partners. Adding the loop diagrams when calculating the Higgs mass, the fermion loop diagrams cancel the boson loop diagrams, and the Higgs mass does not diverge towards infinity. However, this particle-sparticle symmetry somehow has to be broken, since a perfect symmetry gives sparticles with masses equal to their SM partners. No experiment has ever detected a supersymmetric particle, which means that the sparticles are either so heavy that they cannot be seen with the energies currently available at particle accelerators, or that the supersymmetric theories have no foundation in the real, physical world.

Two mechanisms describing this SUSY breaking are the gauge mediated supersymmetry breaking mechanism (GMSB) and the gravity mediated supersymmetry breaking mechanism. The gravity mediated mechanism, which is a supergravity inspired model, assumes that the gaugino (the gauginos are the winos and bino) mass, the scalar masses and the trillinear couplings are equal at the grand unified theory (GUT) scale. In this model, SUSY is broken at a very high scale, a "hidden sector" close to the GUT scale, and communicated to the visible sector through gravitational interactions. GMSB breaks SUSY at only a few hundred TeV scale, with the gauge bosons as the messengers. In the gravity mediated SUSY breaking model the lightest supersymmetric particle (LSP) is the neutralino if the symmetry between the bosons and leptons, often called R-parity which is defined as

$$R_p = (-1)^{3B+L+2j}, \tag{2.19}$$

is conserved. The neutralinos are the physical particles resulting the from mixing of the neutral higgsinos and the neutral gauginos. Assuming conservation of R-parity, the LSP is stable, but with a behavior similar to the neutrino: it will escape through the detectors undetected. This means a large amount of missing energy in the detector. There is no reason for SUSY particles not to show R-parity violating properties, but the R-parity breaking cannot be such that the proton decays, considering the proton lifetime: $\tau_{proton} > 1.6 \times 10^{25}$ years [5].

GMSB models have the gravitino as the LSP and either a neutralino or a sfermion as the next lightest sparticle (NLSP). The decay channels are then either $\tilde{\chi}^0 \to \tilde{g} + \gamma$ or $\tilde{f} \to \tilde{g} + f$.

2.2.1 The two-doublet Higgs Model

The simplest expansion of the Standard Model is to introduce another Higgs doublet. The potential

$$\begin{aligned} V(\phi_1,\phi_2) &= \lambda_1(\phi_1^\dagger\phi_1 - v_1^2)^2 + \lambda_2(\phi_2^\dagger\phi_2 - v_2^2)^2 \\ &+\lambda_3[(\phi_1^\dagger\phi_1 - v_1^2) + (\phi_2^\dagger - v_2^2)]^2 \\ &+\lambda_4[(\phi_1^\dagger\phi_1)(\phi_2^\dagger\phi_2) - (\phi_1^\dagger\phi_2)(\phi_2^\dagger\phi_1) \\ &+\lambda_5[Re(\phi_1^\dagger\phi_2) - v_1v_2\cos\xi]^2 \\ &+\lambda_6[Im(\phi_1^\dagger\phi_2) - v_1v_2\sin\xi]^2, \end{aligned} \tag{2.20}$$

for two scalar doublets ϕ_1 and ϕ_2 spontaneously breaks $SU(2)_L \times U(1)_Y$ down to $U(1)_{EM}$. If all the real parameters λ_i are positive, the vacuum expectation values (VEV's) of the Higgs doublets are:

$$< \phi_1 >= \begin{pmatrix} 0 \\ v_1 \end{pmatrix}, < \phi_2 >= \begin{pmatrix} 0 \\ v_2 e^{i\xi} \end{pmatrix}, \tag{2.21}$$

and the ratio of the vacuum expectation values is $\tan\beta = \frac{v_2}{v_1}$. If $\lambda_5 = \lambda_6$ the phase ξ can be rotated away, and Eq. 2.20 becomes CP-invariant. By performing a spontaneous symmetry breaking, the different physical (and unphysical) particles and their masses are found. The two-doublet Higgs model gives five real, *i.e.* true, physical particles, and three imaginary particles, *i.e.* particles that does not exist anywhere but in the equation. The real particles are the two charged Higgs bosons, $H^\pm = -\phi^\pm\sin\beta + \phi^\pm\cos\beta$, with masses $m_H^\pm = \lambda_4(v_1^2+v_2^2)$, one neutral CP-odd scalar, the A_0 with mass $m_{A_0} = \lambda_6(v_1^2+v_2^2)$, which appears when the imaginary and the real part of the neutral scalar field are split, and finally two CP-even neutral Higgses, which mix through the mixing matrix

$$\mathcal{M} = \begin{pmatrix} 4v_1^2(\lambda_1+\lambda 3) + v_1^2\lambda_5 & (4\lambda_3+\lambda_5)v_1v_2 \\ (4\lambda_3+\lambda_5)v_1v_2 & 4v_2^2(\lambda_2+\lambda_3) + v_1^2\lambda_5 \end{pmatrix}, \tag{2.22}$$

giving the neutral Higgses their physical mass eigenstates

$$H^0 = \sqrt{2}[(Re\phi_1^0 - v_1)\cos\alpha + (Re(\phi_2^0 - v_2)\sin\alpha] \tag{2.23}$$

$$h^0 = \sqrt{2}[-(Re\phi_1^0 - v_1)\sin\alpha + (Re(\phi_2^0 - v_2)\cos\alpha], \tag{2.24}$$

where α is a mixing angle given by the different matrix elements of the mixing matrix 2.22. The masses of the neutral Higgs bosons are given by

$$m^2_{H^0,h^0} = \frac{1}{2}\left[\mathcal{M}_{11} + \mathcal{M}_{22} \pm \sqrt{(\mathcal{M}_{11} - \mathcal{M}_{22})^2 + 4\mathcal{M}_{12}^2}\right] \tag{2.25}$$

The imaginary particles are two charged and one neutral massless Goldstone bosons. The charged Goldstone bosons, $G^\pm = \phi^\pm\cos\beta + \phi\pm\sin\beta$, are the orthogonal partners to the charged Higgs bosons, and the neutral Goldstone boson is the CP-odd partner to the A_0. The Goldstone bosons are removed when the Higgs bosons become real.

2.2.2 The Minimal Supersymmetric Standard Model

In the Minimal Supersymmetric extension of the Standard Model (MSSM), with a scalar, two-doublet Higgs field,

$$H_1 = \begin{pmatrix} \phi_1^0 \\ -\phi_1^- \end{pmatrix}, H_2 = \begin{pmatrix} \phi_2^+ \\ -\phi_2^0 \end{pmatrix}, \tag{2.26}$$

the superpotential Eq. 2.20, including soft supersymmetry breaking terms (MSSM does not fix the SUSY breaking mechanism, both GMSB and gravity mediated SUSY breaking models are allowed), takes this form

$$\begin{aligned} V &= (m_1^2 + |\mu|^2) H_1^{i*} H_1^i + (m_2^2 + |\mu|^2) H_2^{i*} H_2^i + m_{12}^2 (\epsilon_{ij} H_1^i H_2^j + h.c) \\ &\quad + \tfrac{1}{8}(g_2^2 + g_1^2) \left[H_1^{i*} H_1^i - H_2^{j*} H_2^j \right]^2 + \tfrac{1}{2} g_2^2 | H_1^{i*} H_1^i |^2 \end{aligned} \tag{2.27}$$

where the parameters m_1, m_2 and m_{12} have dimension of mass and μ is a SUSY-conserving Higgs mass parameter. MSSM does not, as opposed to other non-minimal models, contain a singlet field N, which breaks SUSY.

The minimization constraints guaranteeing non-zero values for the Higgs vacuum expectation value v_1 and v_2 gives constraints on the λ_i appearing in the general two-doublet Higgs field potential 2.20 and the parameters in the MSSM potential 2.27. Tree-level masses for the different particles found in the general two-doublet model can now be found (demanding that $m_{H^\pm} > m_W$ and no N field):

$$\begin{aligned} m_{A_0}^2 &= m_{H^\pm}^2 - m_W^2 \\ m_{H^0,h^0}^2 &= \frac{1}{2} \left[m_{A_0}^2 + m_Z^2 \pm \sqrt{(m_{A_0}^2 + m_Z^2)^2 - 4 m_Z^2 m_{A_0}^2 \cos^2 2\beta} \right]. \end{aligned} \tag{2.28}$$

Note that none of the five real particles described here, the $H^\pm$, the H^0, the h^0 and the A^0, are supersymmetric particles, but appears as a result of expanding the Higgs field from a one-doublet to a two-doublet model. This means that the five particles have supersymmetric partners, see Table 2.1. These sparticles are weak eigenstates, and thus mix to give the physical mass eigenstates. Mixing between the charged Higgsinos and the charged winos gives the charginos and mixing between the neutral Higgsinos and the neutral wino and bino gives the neutralinos.

2.2.3 Where to look for Supersymmetric particles

Experimentally, the neutralinos and charginos might be the supersymmetric particles that are the most easy to detect, owing to their supposed clean experimental signature [6].

Mixing of the charged gauginos and higgsinos

In a $SU(2)\times U(1)$ model of broken supersymmetry, the gaugino and higgsino mass term in the Lagrangian are given by [6] p.210:

$$\frac{ig}{\sqrt{2}}\left[v_1\tilde{W}^+\tilde{H}_2^+ + v_2\tilde{W}^-\tilde{H}_1^-\right] + M_2\tilde{W}^+\tilde{W}^- - \mu\tilde{H}_1^-\tilde{H}_2^+ + h.c. \qquad (2.29)$$

where $\tilde{W}^\pm$ are the winos, $\tilde{H}_{1,2}^\pm$ are the charged higgsinos, see Table 2.1, v_1 and v_2 are the Higgs VEV's, μ is a HIggs mixing term and M_2 is a gaugino mass term. Defining ψ_j^+ and ψ_j^- as

$$\psi_j^+ = (-i\tilde{W}^+\ \tilde{H}_2^+),\ \psi_j^- = (-i\tilde{W}^-\ \tilde{H}_1^-) \qquad (2.30)$$

with $j = 1, 2$, the mass terms of the Lagrangian, Eq. 2.29, can be written as

$$-\frac{1}{2}(\psi^+\ \psi^-)\begin{pmatrix} 0 & X^T \\ X & 0 \end{pmatrix}\begin{pmatrix} \psi^+ \\ \psi^- \end{pmatrix} + h.c. \qquad (2.31)$$

The matrix X is defined as

$$X = \begin{pmatrix} M & m_W\sqrt{2}\cos\beta \\ m_W\sqrt{2}\sin\beta & \mu \end{pmatrix}. \qquad (2.32)$$

The chargino mass eigenstates, χ^+ and χ^-, can then be found by

$$\chi_i^+ = V_{ij}\psi_j^+,\ \chi_i^- = U_{ij}\psi_j^- \qquad (2.33)$$

where the U and V matrices are chosen such that they diagonalize the matrix X:

$$U^* X V^{-1} = M_D, \qquad (2.34)$$

M_D being a diagonal matrix with non-negative entries. Since these are all 2×2 matrices, analytical expressions are possible when diagonalizing the matrix X. By defining the matrices $O_\pm$

$$O_\pm = \begin{pmatrix} \cos\phi_\pm & \sin\phi_\pm \\ -\sin\phi_\pm & \cos\phi_\pm \end{pmatrix}., \qquad (2.35)$$

where the angles $\phi_\pm$ are defined as

$$\tan 2\phi_- = 2\sqrt{2}m_W\frac{\mu\cos\beta + M_2\sin\beta}{M_2 - \mu^2 + 2m_W\cos 2\beta} \qquad (2.36)$$

$$\tan 2\phi_+ = 2\sqrt{2}m_W\frac{\mu\sin\beta + M_2\cos\beta}{M_2 - \mu^2 - 2m_W\cos 2\beta}, \qquad (2.37)$$

one can find the matrices U and V, assuming that M_2 and μ are real:

$$U = O_-,\ V = \begin{cases} O_+, det\ X \geq 0 \\ \sigma_3 O_-,\ det\ X < 0 \end{cases} \qquad (2.38)$$

The explicit chargino mass terms can be found analytically when using the matrices U and V to diagonalize the matrix X, and are

$$M^2_{\tilde{\chi}^+,\tilde{\chi}^-} = \begin{array}{l} \frac{1}{2}\{M_2^2 + \mu^2 + 2m_W^2 \\ \pm\sqrt{(M_2-\mu^2)^2 + 4m_W^4\cos 2\beta + 4m_W^2(M_2^2+\mu^2+2M_2\mu\sin 2\beta)}\} \end{array} \qquad (2.39)$$

Mixing of the neutral gauginos and higgsinos

The mass eigenstates of the neutralinos are more complicated to calculate than the mass eigenstates of the charginos, since the neutralino mixing matrix include four charge neutral particles, not counting the neutral particle appearing if the scalar field N is included, and not just two charged particles as in the chargino case. In the basis

$$\psi^0 = (\tilde{B}, \tilde{W}^3, \tilde{H}_1^0, \tilde{H}_2^0) \tag{2.40}$$

the neutral fields mass terms are [6] p.215

$$\begin{array}{l} \frac{1}{2}\tilde{W}^3(v_1\tilde{H}_1^0 - v_2\tilde{H}_2^0) - \frac{1}{2}ig_1\tilde{B}(v_1\tilde{H}_1^0 - v_2\tilde{H}_2^0) \\ +\frac{1}{2}M_2\tilde{W}^3\tilde{W}^3 + \frac{1}{2}M_1\tilde{W}^3\tilde{W}^3 + \mu\tilde{H}_1^0\tilde{H}_2^0 + h.c. \end{array} \tag{2.41}$$

The prediction that the gaugino masses unite at the GUT scale have been used in the calculations of Eq. 2.41. The gaugino masses M_1 and M_2 are then related by

$$M_1 = \frac{5}{3}\frac{g_1^2}{g_2^2}M_2 \simeq 0.5M_2. \tag{2.42}$$

Using Eq. 2.40, the mass terms of Eq. 2.41 can be written

$$-\frac{1}{2}(\psi^0)^T Y \psi^0 + h.c. \tag{2.43}$$

where the matrix Y is defined as

$$Y = \begin{pmatrix} M_2 & 0 & -m_Z \sin\beta \sin\theta_W & m_Z \cos\beta \sin\theta_W \\ 0 & M_1 & m_Z \sin\beta \cos\theta_W & -m_Z \cos\beta \cos\theta_W \\ -m_Z \sin\beta \sin\theta_W & m_Z \sin\beta \cos\theta_W & 0 & -\mu \\ m_Z \cos\beta \sin\theta_W & m_Z \sin\beta \sin\theta_W & -\mu & 0 \end{pmatrix} \tag{2.44}$$

where M_1 and M_2 are the gaugino masses, μ is the Higgs mixing term and the off-diagonal terms describe the coupling of the higgsinos to the gauginos. v_1 and v_2 are the ratio of the vacuum expectation values of the two Higgses. In the expression above, $\tilde{W}^3$ and $\tilde{B}$ are the convention, but $\tilde{Z}^0$ and $\tilde{\gamma}$ could equally well have been used. The neutralino mass eigenstates are found by defining

$$\tilde{\chi}_i^0 = N_{ij}\psi_j^0, j = 1, \ldots, 4 \tag{2.45}$$

where N is a unitary matrix that diagonalize the mass matrix Y

$$N^* Y N^{-1} = N_D \tag{2.46}$$

in the same manner as the matrices U and V diagonalize the charged gaugino mass matrix.

However, this mass matrix is so complicated to diagonalize that an analytical expression is not possible to obtain, and numerical methods have to be used.

Parameter determination

Since supersymmetric theories have the gaugino masses and the mixing angles $\tan\beta$ and α as unknown parameters, they have to be decided by experiment. This means that in a search for supersymmetric particles, one has to look for different decay channels, since it is unknown which particle that is the LSP.

Decays of W bosons into neutralinos and charginos

Ref. [7] discuss the possibility of $e^+e^- \to W^+W^-$ collisions with one W decaying into a lepton-neutrino pair or a quark-antiquark pair, *i.e.* into Standard Model particles, and the other W decaying into a chargino-neutralino pair, $W^\pm \to \tilde{\chi}_i^+ \tilde{\chi}_j^0$ with the chargino decaying subsequently into a charged lepton and a selectron pair, $\tilde{\chi}_i^\pm \to \tilde{\nu}_l l^\pm$. The problem with this decay channel is that the sneutrino, being either the LSP or decaying into a neutrino and the lightest neutralino, is invisible in the detector and the energy of the leptons are so low that they will escape through the detector undetected. A "blind spot" results from this problem, making the detection or exclusion of supersymmetric particles difficult. Due to this blind spot, the charginos might be as light as 45 GeV [8] without being detected. In [9] and Chapter 7 a procedure to solve this problem is described.

With the assumption that the wino and bino masses unite at the GUT scale, see Eq. 2.42, the partial width of W bosons decaying into any chargino-neutralino pair is given by [7]:

$$\begin{aligned}&\Gamma(W^+ \to \chi_i^+ \chi_j^0) = \frac{G_F m_W^2 \lambda_{ij}^{1/2}}{6\sqrt{2}\pi} \\ &\times\{[2 - \kappa_i^2 - \kappa_j^2 - (\kappa_i^2 - \kappa_j^2)^2](Q_{Lij}^2 + Q_{Rij}^2) \\ &+12\kappa_i\kappa_j Q_{Lij} Q_{Rij}\}\end{aligned} \tag{2.47}$$

where $i = 1, 2$ denotes the two different charginos, $j = 1, \ldots, 4$ denotes the four different neutralinos, κ_i is the ratio between the mass of the chargino in question and the W mass, κ_j is the ratio between the mass of the neutralino and the W mass. λ_{ij}, a two-body phase space factor, is defined as $\lambda_{ij} = (1 - \kappa_i^2 - \kappa_j^2)^2 - 4\kappa_i^2\kappa_j^2$, G_F is the Fermi coupling constant and Q_{Lij} and Q_{Rij} are the couplings of the W to the charginos and neutralinos, defined as the matrix elements

$$Q_{Lij} = Z_{j2}V_{i1} - \frac{1}{\sqrt{2}} N_{j4} V_{i2} \tag{2.48}$$

$$Q_{Rij} = Z_{j2}U_{i1} - \frac{1}{\sqrt{2}} N_{j3} U_{i2}. \tag{2.49}$$

U and V are the matrices that diagonalize the charged gaugino mass matrix, recall Eq. 2.38, and N is the mixing matrix in the neutralino sector, *i.e.* the matrix that diagonalizes the neutral gaugino mass matrix, recall Eq. 2.46.

Chapter 3

The DELPHI experiment

The European center for Particle physics, CERN, consists of several particle accelerators, see Fig. 3.1. When particles are going to be accelerated into the Large Electron and Positron collider LEP, they are first accelerated in the smaller rings PS, the Proton Synchrotron, and SPS, the Super Proton Synchrotron, before they have enough momentum to be injected into the large LEP collider.

3.1 The LEP accelerator

The largest accelerator at CERN, the Large Electron and Positron (LEP) collider, accelerates electrons and positrons in opposite directions inside a vacuum tube. This pipe is placed in a tunnel 100 meters below the earth's surface.

Large detectors are placed at four of the beam crossings around the LEP ring, the DELPHI, ALEPH, L3 and OPAL detectors, see Fig. 3.1. Since each of the detectors are designed differently from the others, they all have their special strengths when it comes to *e.g.* particle detection.

LEP1 started running in 1990, and was upgraded to LEP200 in 1996. The total integrated luminosity per year and the center-of-mass energies for the different stages of the two phases are listed in Table 3.1.

	LEP1						LEP200		
	1990	1991	1992	1993	1994	1995	1996	1997	1998
$\int \mathcal{L}$	7.6	17.3	28.6	40	64.4	46.1	10/10	64	158
$\sqrt{s}$	130/136						161/172	183	189

Table 3.1: The total integrated luminosity pr. year in pb^{-1} and center-of-mass-energies in GeV for the two phases of LEP.

3.2 The DELPHI experiment

The **DE**ctector with **L**epton, **P**hoton and **H**adron **I**dentification (DELPHI) is actually a collection of many smaller detectors, each with its special purpose. An overview of the detector is shown in Figure 3.2. The detector consists of a barrel part and two endcap regions which covers most of the solid angle. The different subdetectors can be classified according to their general purpose, and are [10] and [11]:

- Charged Particle Tracking detectors:
  - **The Vertex Detector** (VD)
    is the detector nearest the collision point. Its task is to detect very short-lived particles.
  - **The Inner Detector** (ID)
    gives intermediate precision positions and trigger information.
  - **The Time Projection Chamber** (TPC)
    is the principal tracking device in the DELPHI detector, detecting particles that ionize the gas in the chamber. It also provides identification of charged particles by $\mathrm{d}E/\mathrm{d}X$ measurements.
  - **The Outer Detector** (OD)
    consists of five layers of drift tubes, and gives a final precise position and direction measurement after the RICH (described later).
  - **The Forward Chamber A** (FCA)
    provides tracking and triggering in the forward direction, and covers polar angles from 11^o to 32^o and 148^o to 169^o. The FCA is placed before the Forward RICH.
  - **The Forward Chamber B** (FCB)
    is a drift chamber that provides precise tracking in the forward direction. It is placed after the Forward RICH, and covers polar angles between 11^0 to 36^o and 144^o to 169^o.
  - **The Very Forward Tracker** (VFT)
    is located at both sides of the vertex detectors, and covers polar angles from 10^o to 25^o.
  - **The Muon Chambers** (MUC)
    are the Barrel Muon Chambers, the Forward Muon Chambers and the Surround Muon Chambers, and provide identification of muons. Since muons are the only charged particles that can penetrate both the calorimeters, the MUC are placed farthest away from the collision point.
- Electromagnetic calorimeters
  mainly measures the energies of photons and electrons.

- **The High-Density Projection chamber** (HPC)
  is an electromagnetic calorimeter consisting of 41 layers of lead separated by gas.
- **The Forward ElectroMagnetic Calorimeter** (FEMC)
  consists of two discs (one on each end of the detector) 5 meters in diameter. The discs are made of lead-glass blocks.

- Hadron calorimeter
  - **The Hadron Calorimeter** (HAC)
    Has as its main purpose measurements of the energy of charged and neutral hadrons. The HAC is made up of a barrel part and two endcap parts. The barrel part consists of 24 sections with 20 layers of wire chamber detectors. The wire chambers are filled with an argon (10 %), CO_2 (60 %), i-butane (30 %) mixture, and vary in length from 40 to 410 cm. For each layer there are 5 cm iron plates. The endcap parts are similar to the barrel part, but consists of 19 layers of detectors. All together, the HAC consists of ca. 19000 detectors.

- Charged hadron identification

  is performed with two Ring Imaging Cherenkow Counters (RICH) detectors, one in each endcap region, the Forward RICH, and one in the barrel region, the Barrel RICH. These detectors are able to detect particles exiting the detectors at all angles. The RICH contains two different radiators with different refractive indices. The liquid radiator is used for detection of protons, π-mesons and kaons with momentum between 0.7 to 9 GeV, and the gas radiator is used for detection of particles with momentum between 2.5 and 25 GeV.

- Luminosity measurement

  is done by counting the number of events of a high statistic process with clear experimental fingerprints and a cross section that is theoretically well-known. At DELPHI the chosen process is Bhabha scattering ($e^+e^- \rightarrow e^+e^-$) at small angles.
  - **The Small angle TIle Calorimeter** (STIC)
    is a sampling lead-scintillator calorimeter, placed 2.2 meters on each side of the collision center.
  - **The Very Small Angle Tagger** (VSAT)

is build up of 12 layers of a wolfram plate and silicon detector sandwich. The detector is placed 7.7 meters from the collision center, and measures particles leaving the detector in a very forward direction, 6 to 8 mrad.

A superconducting solenoid, parallel to the beam pipe, makes a strong, uniform magnetic field of 1.2 Tesla, bends the path of all charged particles in the detector into helixes. This makes momentum measurements possible. The solenoid is 7.4 meters long and has an inner radius of 2.6 meters. Liquid helium cools the solenoid to 4.5 Kelvin, in order to make it superconducting.

The collection of these subdetectors makes DELPHI a detector with emphasis on strong particle identification and precise vertex determination. All together, the DELPHI detector is more than 10 meters long and has a radius of more than 5 meters, and weighs over 3500 tons.

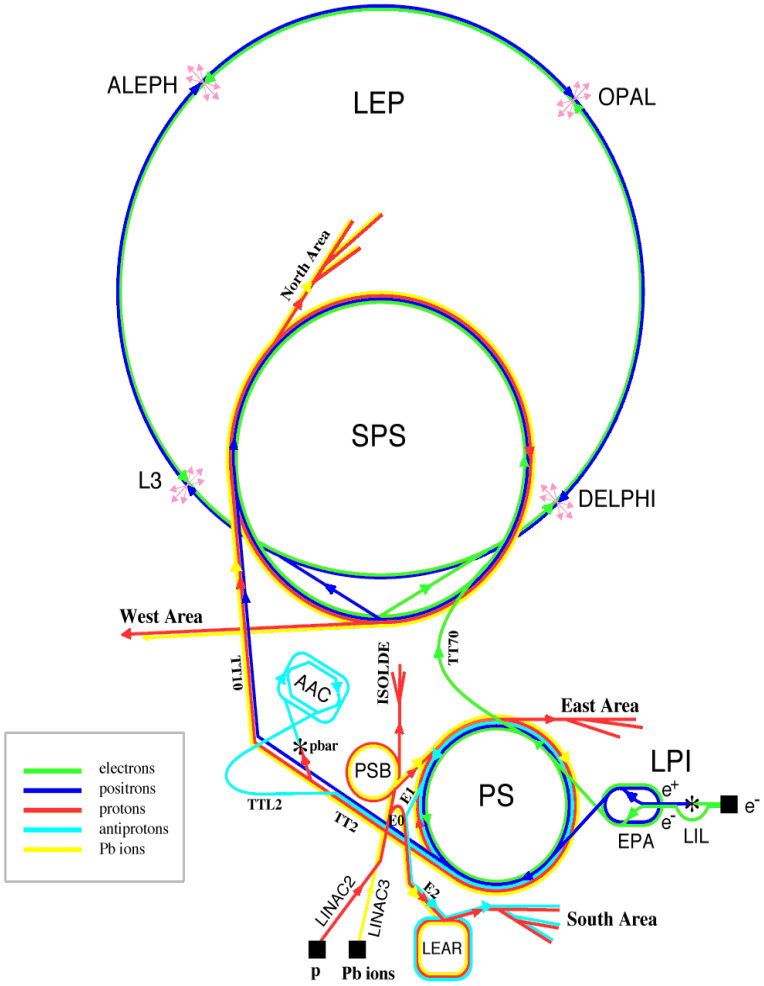

Figure 3.1: The different accelerators and experiments at CERN.

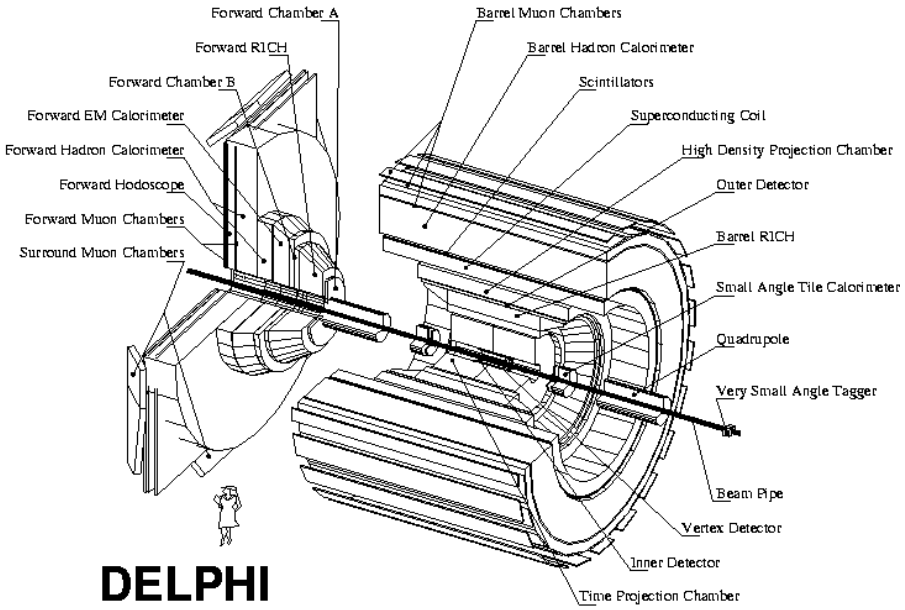

Figure 3.2: The DELPHI detector, with all its subdetectors. The figure shows the detector when one of the endcaps is pulled away from the detector.

Chapter 4

Statistical treatment of search experiments

Although the detectors and accelerators described in the Chapter 3 are the main tools for making discoveries in particle physics, computer treatment of the physics being tested is an important part of the search for new physics. The lifetime of particles decaying through the strong or the electromagnetic forces have lifetimes less than 10^{-16} seconds, which is so short that the detectors are not able to detect the particles before they decay into other particles with longer lifetimes. It is these particles and their trajectories and momenta that are detected. Since the Standard Model Higgs boson is a neutral particle, it has to decay into charged particles before the detectors can "see" the particle, as with any other neutral particle. A large part of the computer analysis is the simulation of the detector, in order to find out how particles inside the detector behaves. When one has determined which processes are expected to happen in the detector, one can compare the observed data to what is expected to have taken place in the detector.

However, this is not enough. The signal from the detector saying a particle just hit some of the subdetectors might not be a true signal, but can either be a result of other Standard Model processes looking like the signal the physicists are looking for, it might be cosmic ray induced background noise or it might be electronic noise in the detector, although this very rarely is a problem.

4.1 Confidence limits and hypothesis testing of search results

When some event have satisfied certain selection criteria of the search, one has to decide whether the detector has actually seen a true signal or if some other processes has produced a fake signal. This is done by a hypothesis test, where the agreement between the observed data and the predicted

probabilities, *i.e.* the *signal* which is found by *e.g.* Monte Carlo simulations, is computed.

The normal procedure is to define the hypothesis saying the signal is absent as the *null* hypothesis, and the *alternate* hypothesis as saying the signal is a true one. Instead of just giving a yes-or-no answer when analyzing the hypotheses, the strength of the discovery or exclusion of the hypothesis is stated as a *confidence level*.

The probability density function (p.d.f.) is a function describing how the probability of having an outcome X in an infinitesimal interval, $[x, x+dx]$, varies over the range of possible outcomes. Thus the probability density function $f(X)$ is defined as

$$P(X \in [x, x+dx]) = f(x)dx. \tag{4.1}$$

To be able to compare the observed data to the hypothesis, a *test statistic*, which is a function of the observed data, is selected. The test statistic is constructed in such a way that it will increase if the experiment gets more like a true signal, and decrease if the experiment gets less like a true signal and more background-like.

Unfortunately it is not possible to turn off the background in the detector, but one will have to compare a hypothesis where both signal and background noise are included to the background-only hypothesis. The *background-only* hypothesis is a prediction of what is seen in the detectors had there been only background events.

The confidence in the *signal+background* hypothesis is given by the probability of the test-statistic to be less than or equal to the observed value X_{obs}

$$CL_{sb} = P_{s+b}(X \leq X_{obs}), \tag{4.2}$$

where P_{s+b} is found by integrating the probability density function from 0 to the observed value, $P_{s+b}(X \leq X_{obs}) = \int_0^{X_{obs}} f_{s+b}(x)dx$.

Equally, the confidence level of the *background only* hypothesis is

$$CL_b = P_b(X \leq X_{obs}), \tag{4.3}$$

where P_b is found by integrating the probability density function for the *background only* hypothesis from zero to the observed value, $P_b = \int_0^{X_{obs}} f_b(x)dx$, just as in the *signal+background* case.

To give a picture of what would have been seen in the detector had there been *no* background processes in the detector, the confidence of the *signal+background* hypothesis is normalized to the *background only* hypothesis to form what is chosen to be defined as the confidence of the *signal only* hypothesis.

$$CL_s \equiv \frac{CL_{s+b}}{CL_b}. \tag{4.4}$$

CL_s is not a true confidence [12], but due to its similarity, one says that the signal hypothesis is excluded at the confidence level CL when

$$1 - CL_s \leq CL. \tag{4.5}$$

4.2 The Likelihood Ratio Test Statistic

Given a hypothesis with a p.d.f $f(x)$, the probability of having the first of several outcomes in the interval $[x_1, x_1 + dx_1]$ is $f(x_1)dx_1$, the probability of having the second outcome in the interval $[x_2, x_2 + dx_2]$ is $f(x_2)dx_2$, [13], and so on. Assuming that all measurements are independent, *i.e.* there is no correlation between the different values x_i, the expression for all the observed events is:

$$P(\forall i : x_i \in [x_i, x_i + dx_i]) = \prod_{i=1}^{n} f(x_i)dx_i. \tag{4.6}$$

This expression motivates the making of the *likelihood function* [1], also known as the *method of betting odds*:

$$\mathcal{L} = \prod_{i=1}^{n} f(x_i), \tag{4.7}$$

which, in reality, is just the joint probability density function of all the observed values. In a hypothesis test one can as a test-statistic use the ratio of the likelihood functions of the two hypotheses, the *likelihood ratio*

$$Q = \frac{\mathcal{L}(\vec{X}; A)}{\mathcal{L}(\vec{X}; B)}, \tag{4.8}$$

where $\vec{X}$ is the space of possible outcomes, and A and B are parameters of the hypotheses being tested. Since the likelihood ratio maximizes the probability of excluding a false hypothesis [14], it is commonly used as a test statistic.

An appropriate likelihood ratio for searches in particle physics is

$$Q = \frac{\mathcal{L}(\vec{X}; s + b)}{\mathcal{L}(\vec{X}; b)}, \tag{4.9}$$

where s and b are the integrated signal and background rates for the hypotheses being tested. Since these parameters share the same space of outcomes, $\vec{X}$ is dropped from the expression for simplicity.

[1] This also motivates the *method of maximum likelihood*, where the parameters of the hypothesis are found by differentiating the likelihood function with respect to its estimators θ: $\frac{\partial \mathcal{L}}{\partial \theta} = 0$.

If the search includes some measurements on the experimental candidates, *e.g.* the mass distribution of the observed candidates, the likelihood function of the hypothesis has to include more information than just the number of observed events. This information is given in the form of a discriminating variable.

Since the Poisson distribution describes processes where the probability of each event is small and constant, *i.e.* is independent with respect to time and space, it is well suited in the search for new particles, which normally have few, if any, observed events. In a search with N_{chan} distinct search channels, the likelihood ratio takes this form:

$$Q = \frac{\prod_{i=1}^{N_{chan}} \frac{e^{-(s_i+b_i)}(s_i+b_i)^{n_i}}{n_i!} \prod_{j=1}^{n_i} \frac{s_i S_i(x_{ij})+b_i B_i(x_{ij})}{s_i+b_i}}{\prod_{i=1}^{N_{chan}} \frac{e^{-b_i} b_i^{n_i}}{n_i}}, \tag{4.10}$$

with n_i as the number of observed candidates in each channel, x_{ij} is the discriminating variable, in case more information than just the number of observed events in each channel is known, and $S_i(x_{ij})$ and $B_i(x_{ij})$ are the probability density functions of the discriminating variable for respectively the signal hypothesis and the background hypothesis. This expression can be simplified to

$$Q = e^{-s_{tot}} \prod_{i=1}^{N_{chan}} \prod_{j=1}^{n_i} \left(1 + \frac{s_i S_i(x_{ij})}{b_i B_i(x_{ij})}\right). \tag{4.11}$$

This likelihood ratio can, if the p.d.f.'s of the discriminating variable is equal for signal and background, or if there haven't been measured a p.d.f. of the discriminating variable, be simplified even more:

$$Q = e^{-s_{tot}} \prod_{i=1}^{N_{chan}} \prod_{j=1}^{n_i} \left(1 + \frac{s_i}{b_i}\right). \tag{4.12}$$

To obtain a linear expression, one can take the logarithm of Eq. 4.12:

$$\ln(Q) = -s_{tot} + \sum_{k=1}^{N_{chan}} n_k w_k, \tag{4.13}$$

where the weight w_k is given by

$$w_k = \ln\left(1 + \frac{s_i}{b_i}\right). \tag{4.14}$$

This means that the likelihood ratio is more or less a method of counting weighted events.

In this section, there have been made no difference between *a posterior* and *a prior* probability, [14].

When one has knowledge of the experiment before doing it, one has *a prior* probabilities. An example of this would be tossing a coin: it can land on either side, with equal probabilities, or it can land on the edge, which is fairly improbable.

If, for some reason, the *a prior* probability can not be known in advance, the *a posterior* probability is found by performing the experiment. The *a posterior* probability includes experimental uncertainties, while the *a prior* probability is known exactly. To decrease the experimental uncertainties of the *a posterior* probabilities, the experiment has to be performed several times (to obtain an uncertainty of zero, the experiment has to be performed infinitely many times).

Strictly speaking, the term likelihood ratio described above applies only to *a posteriori* probabilities, but has been used with *a priori* probabilities for convenience.

4.3 When analytical solutions are not possible

In a multichannel search where the probability density function also includes discriminating variable in addition to the number of observed events, finding an analytic solution of the likelihood probability distribution function, as described in the previous section, is technically impossible. If one tries to solve Eq. 4.10 for a search with n channels and m possible outcomes for each channel, one have to solve an expression of order $\mathcal{O}(n^m)$ terms [15]. A multichannel search might have as many as 5000 channels, when counting the different mass bins in each search channel as a single channel. Restricting the number of possible outcomes to zero, one or two candidates in any bin, this gives an expression of 3^{5000} terms to solve. In the 1998 DELPHI Higgs boson search, one will easily have to solve expressions with more than 10^{5000} term.

To solve this problem, the probability density functions have to be found non-analytically. One possibility is Monte Carlo generation of the p.d.f. The confidence limit is then the fraction of the Monte Carlo experiments with $Q \leq Q_{obs}$. Another is described in the following section.

4.3.1 Semianalytic computation of the p.d.f.

In this alternative method, the probability distribution function is found by looking at the probability of different outcomes in the different channels and then combining these probabilities. The meaning of "channel" is the same as in the previous section, it can either be a search channel in a search with number of observed events as the only information, or it can *e.g.* be a mass bin in a search with mass information in addition to the number of observed candidates. A schematic picture of how the p.d.f. is created is

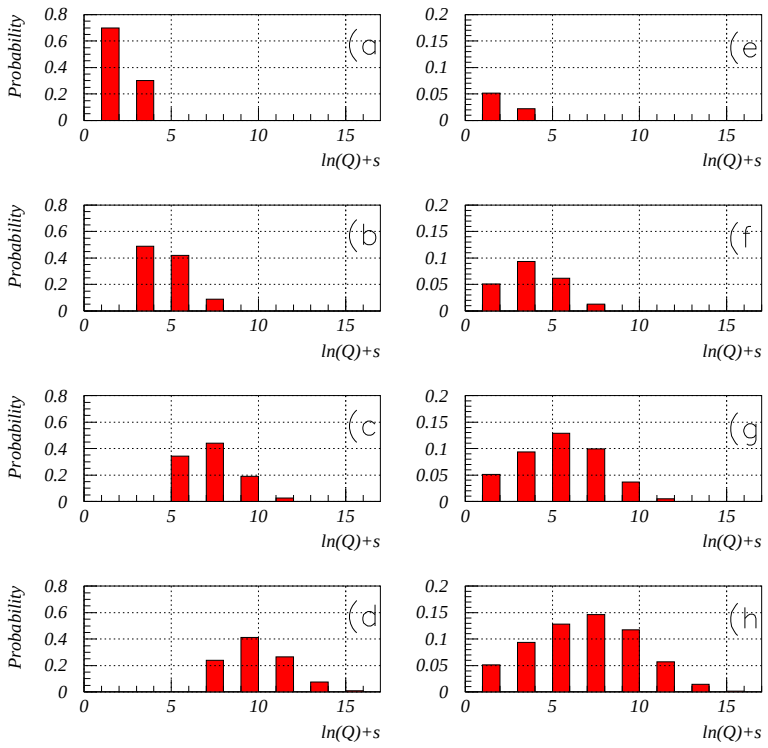

Figure 4.1: The calculation of the p.d.f. The figures (a) through (d) shows the different combinations of respectively one, two, three and four candidates. Figures (e) through (h) shows the cumulative result for respectively one, one and two, one, two and three and finally one, two, three and four candidates.

shown in Fig. 4.1. Each channel has its own likelihood ratio, and are sorted with respect to this weight, as in Eq. 4.14.

The first step of calculating the p.d.f. is finding the different possible combinations for one candidate, two candidates, three, four, etc. The axis of Fig. 4.1 are the probability of having an event in the different channels along the y-axis, and the weight of the channels, Eq. 4.14, along the x-axis. The weights are given by the *log* likelihood, and are added instead of multiplied. As an example in a very simple search with two channels, see Fig. 4.2, when finding the different combinations for two candidates, the two candidates can be found either both in the channel with the smallest weight, or they can be found one in each channel (this contribution is multiplied with two since the probability for one candidate in one channel and the other candidate in the other channel is equal to the probability of having the candidates found in the other channel) or they can both be found in the channel with the largest weight. Each possible combination of candidates has one one weight, which

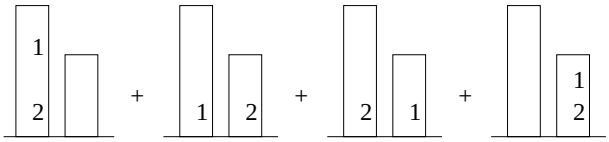

Figure 4.2: The distribution of two candidates in a two-channel search; the numbers shows the different candidates, and the boxes are the different search channels. The higher a box, the larger the probability of having an event in this channel. The total distribution for two candidates is the sum of the different combinations.

is found by summing the weight of the channels where the candidates are, and one probability, which is found by multiplying the probabilities of the different channels.

The second step is to multiply each of these distribution with the corresponding Poisson probability, *e.g* the different possible combinations for one candidate are multiplied with the Poisson probability for one candidate, the different combinations for two candidates are multiplied with the Poisson probability for two candidates, and on.

The third step is to add the combinations, which now are multiplied with the Poisson probability. The number of candidates combined decides how accurate the distribution is. When to stop combining will then be a question of how much time to compute is available and how precise the distribution has to be.

The confidence limit is then found by integrating the computed distribution from zero up to the point given by the observed events, which is found by multiplying the number of observed events in each channel with the weight of that channel, and then summing these weighted candidates:

$$Q_{obs} = \sum_{i=1}^{N_{chan}} \ln(1 + \frac{s_i}{b_i}) n_i^{obs} \tag{4.15}$$

with n_i^{obs} as the number of observed events in channel number i.

A simple implementation utilizing this method is given in appendix A, including subroutines to deal with the mass info from the `DELPHI` Higgs boson search.

4.4 Discovery

If one is interested in whether or not a signal has been discovered,*i.e.* that the observation cannot be explained by background processes, there are much stricter demands on the signal than in the case of hypotheses exclusion. A common way to define the discovery region [16] p. 17, is to demand

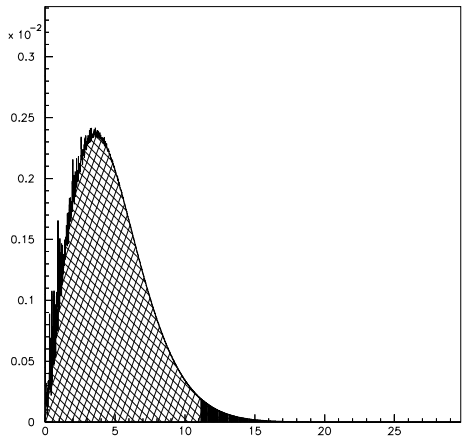

Figure 4.3: One can claim discovery if the area of the *background only* hypotheses, represented by the checked area, left of the observed event is larger than $1 - 5.7 \times 10^{-7}$.

that the probability of the background creating the observation is less than the probability of having a 5 standard deviations fluctuation in a Gaussian distribution, *i.e.* that the probability of background processes being responsible for the observation is less than 5.7×10^{-7}.

The signal also needs to be found where it is expected to be found. If it is not, one has found something that is not created by background processes, but since the signal hypotheses does not predict the signal, it is not a confirmation of the hypotheses.

Chapter 5

The search for the Higgs boson

In this chapter a short description of the 1998 DELPHI Higgs boson search will be given. The full analysis is found in Ref. [17], and although [17] describe both the search for SM and MSSM Higgs bosons, only the search for SM Higgs boson will be described here.

The data were taken at an average center-of-mass energy of $\sqrt{s}$=183 GeV, with an integrated luminosity of 54.0$\pm$0.5 pb^{-1}.

At LEP200 the main Higgs production channel is the $e^+e^- \rightarrow ZH$ channel, see Fig. 5.1 with $H\mu^+\mu^-$, He^+e^- and the $H\nu\bar{\nu}$ channel and channels with jets and taus or purely hadronic channels as the main decay channels of the Higgs and the Z. The analysis has been optimized for events where the Higgs boson either decays into a $\tau^+\tau^-$ pair or into $b\bar{b}$ events, since at the Higgs boson masses searched for $b\bar{b}$ dominates the background, which makes b-tagging important. With a Higgs boson mass of 85 GeV, the branching ratio for Higgs boson decaying into a $b\bar{b}$ pair is approximately 90%, and for Higgs boson decaying into a $\tau^+\tau^-$ pair the branching ratio is approximately 8% [18].

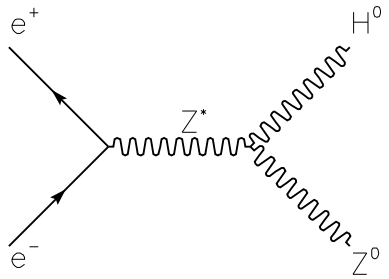

Figure 5.1: The dominant Higgs production channel at LEP200.

5.1 Common features for all channels

In the analysis of [17], there is a set of selection criteria that are common for all events, in addition to decay channel specific selection cuts. The common features are listed below.

5.1.1 Particle selection

In all the decay channels, charged tracks are selected if they have a momentum greater than 100 MeV and if they originate from the collision center (*i.e.* within 10 cm from the interaction center along the beam pipe and within 4 cm in the transverse direction). Neutral particles are found either as energy clusters in the calorimeters or as reconstructed vertices in the tracking volume. Neutral particles found in the calorimeter are selected if the energy is greater than 200 MeV, and neutral particles found in the tracking volume (*i.e.* hadronical energy clusters) are selected if the energy of the cluster is greater than 500 MeV.

5.1.2 b-tagging

The b-tagging has been performed using a method which combine the differences between events containing b-quarks and other events in one single variable x_b^i, see Ref. [19].

The Jet lifetime probability P_j^+ is the probability that the jet correspond to the primary vertex. For a b-event, this probability is smaller that for events with lighter quarks.

The distribution of *the effective mass* of the particles in the secondary vertex M_s is higher for b-events than for the other events.

The distribution of *the rapidity* of the tracks included in the secondary vertex with respect to the jet R_s^{tr}direction is normally lower for b-events than for c-events, since B hadrons are heavier and has a higher multiplicity.

The distribution of *the fraction of charged energy* of the jet included in the secondary vertex X_s^{ch} is for b-events determined by a fragmentation function $f(b \to B)$. This fragmentation function is harder than the equivalent function for c-events. This tag has the weakest tagging power of the variables, since the distributions for b-events almost overlaps the distributions for events with other quark flavors.

Compared to other b-tagging method, where only the impact parameters are taken into consideration, this method provides better rejection of background.

5.1.3 Constrained fits

To extract the Higgs mass two kinds of constrained mass fits have been used: '4-C' fit if only total energy and momentum conservation have been imposed,

and '5-C' fit if the Z mass or the shape of the Z resonance is required as well. In [17] this procedure was also often used to reduce background.

5.1.4 Analysis optimization

The efficiency of each channel has been set in such a way that the sensitivity of the combination is maximized. The working point for each channel is given by the point of the efficiency versus background plot giving the smallest expected signal confidence. This procedure is performed one channel after another, and finally a global optimization, where all channels are optimized together, is performed.

The analysis of Ref. [17] has been divided by the different decay channels of the Higgs boson and the Z boson.

5.2 Searches in events with jets and electrons or muons

The He^+e^- and $H\mu^+\mu^-$ decay channels combined represent 6.7% of the final HZ states.

Muon identification is mainly provided by an algorithm which relies on the association of charged particle tracks to the signals in the barrel and forward muon chambers.

Electron identification is provided by an algorithm that is tuned for efficiency and not purity, since electrons in the HZ channel are expected to be well isolated. Efficiency of this algorithm is 94%, but with a probability of misidentificating a pion as an electron of 16%. This misidentification probability can be lowered to 13% by accepting only tracks associated with electromagnetic showers. This, however, reduces the efficiency to 83%.

In the electron channel events have to consist of five or more charged particles, where two must have a momentum greater than 10 GeV, and the total energy of the event must be more than $0.12\sqrt{s}$.

Events in the muon channel have to have at least four charged particles, and the total energy of the charged particles must be over $0.30\sqrt{s}$. In addition, the total energy in the barrel electromagnetic calorimeter must be less than 100 GeV.

5.3 Searches in events with jets and missing energy

This channel, where the missing energy is due to neutrinos escaping undetected through the detectors, represents 20% of the final HZ states. The experimental signature of this decay channel is a pair of acollinear jets, with a recoiling mass close to the expected mass of $\mathrm{Z} \to \nu\bar{\nu}$ decays.

In order for an event to be selected, it has to consist of at least nine charged particles and the total energy of the charged particles has to be larger than $0.1\sqrt{s}$.

To quantify the differences between the Higgs signal and the background processes, a multidimensional, iterative discriminant analysis was used.

5.4 Searches in events with jets and taus

The experimental fingerprint of this decay channel is two jets and two isolated taus, and 8.5% of all final HZ states end up in this channel. Preselected hadronic events in this channel contain at least seven charged particles and, either a total energy carried by the charged particles greater than $0.15\sqrt{s}$, or a total energy greater than $0.30\sqrt{s}$ and forward and backward energies greater than $0.03\sqrt{s}$.

In this channel, either the H or the Z can decay into the $\tau^+\tau^-$ pair. If the Higgs decays into the τ's, the mass of the τ pair must be high, since the search is for Higgs boson with high mass, and the mass of the jets to be close to Z-mass. On the other hand, if the Z decays into the τ's, the Higgs decays mostly into b-events, and thus b-tagging is a powerful tool against background in this decay channel.

5.5 Searches in events with purely hadronic jets

The preselection, which is equal for all four-jet events, attempts to reduce the $q\bar{q}(\gamma)$ background events while keeping most of the Higgs signal. An event is selected if it contains at least 18 charged particles, a total energy above $0.6\sqrt{s}$ and a total neutral energy less than $0.5\sqrt{s}$. In order to exclude events where an on-shell Z is produced with a photon, no photons with energy above 30 GeV are allowed in the event.

After the preselection, a probabilistic analysis was used. To reduce the main background processes, both b-tagging, topological and kinematical information was used.

5.6 Results of the analysis

As can be seen from Table 5.1, there was no evidence of Higgs bosons in any of the search channels, which means that instead of claiming a discovery, there has been set an exclusion limit on the Higgs mass. In [17] this translates to a lower limit on the mass of the SM Higgs boson of 85.7 GeV at 95 % CL. The observed CL_b and CL_s together with the expected CL_s, computed with `SA_COUNTING`, see Appendix A, is shown in Figure 5.2. In Chapter 6, this analysis will be used to compare three different methods of semianalytic confidence limit calculations.

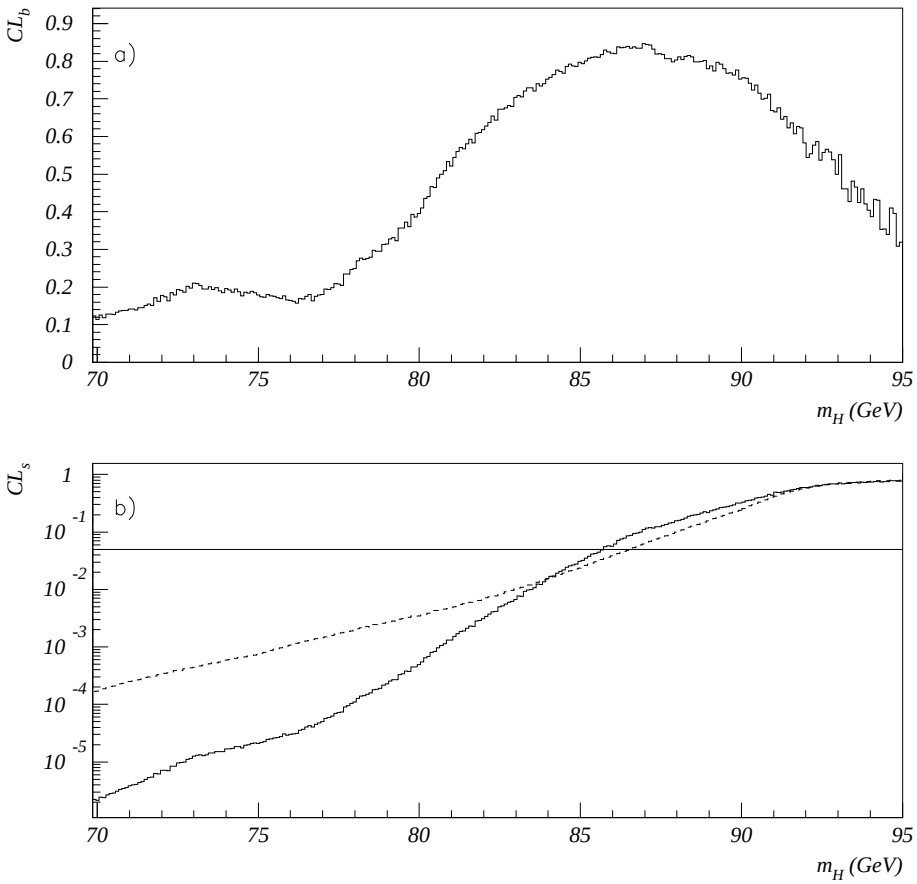

Figure 5.2: Figure (a) shows the observed confidence of the background hypothesis, CL_b. The solid line of (b) is the observed confidence of the signal hypothesis CL_s^{obs}, while the doted line shows the expected confidence.

Channel	Data	Total background	Total sim. signal
$H\mu^+\mu^-$	2	$0.49\pm0.06\pm0.17$	0.43
He^+e^-	1	$0.68\pm0.12^{+0.09}_{-0.10}$	0.26
$H\nu\bar{\nu}$	1	$0.50\pm0.08\pm0.10$	1.25
$H\tau^+\tau^-$	1	$0.74\pm0.09\pm0.08$	0.25
$Z\tau^+\tau^-$	0	$0.34\pm0.07\pm0.04$	0.12
$Hq\bar{q}$	1	$3.74\pm0.20\pm0.18$	5.18

Table 5.1: Data, expected background and simulated signals after all cuts and selections for m_H=85 GeV and $\sqrt{s}$=183 GeV.

Chapter 6

Comparison of three different semianalytic implementations

In this chapter a comparison of four different implementations calculating confidence limits will be described. These implementations have been used to analyze data from the 1998 DELPHI Higgs boson search, described in Chapter 5.

6.1 Differences of the implementations

Three different implementations of the statistical method mentioned in Chapter 4 have been developed: `SA_COUNTING`, see Appendix A, `E_CLS` [15] and `ALRMC_HIST` [12]. Each of these implementations has its own set of strengths and weaknesses. The Monte Carlo routine `ALRMC` has been used to compare the semianalytic implementations.

`ALRMC_` and `SA_COUNTING` combine *all* the different channels at once, *i.e.* they start with the different outcomes for the probability of having one candidate of all the channels, then find the different possible outcomes for two combinations for all the channels, and so on until the distribution has reached almost unity. `E_CLS` starts with the two channels having the smallest signal-to-background ratio, and finds all the different possible combinations for these two channels for as many candidates as it takes to get the accumulated distribution close to 1.0. `ALRMC_HIST` and `SA_COUNTING` compute the distributions until the integrated background p.d.f. has reached 0.999999, while `E_CLS` has a default setting of 0.999. If one needs to compute the p.d.f.'s more or less accurately, changing this number is easy. `E_CLS` just needs a change of a configuration file, while `ALRMC_HIST` and `SA_COUNTING` need a small change of the code and a recompiling.

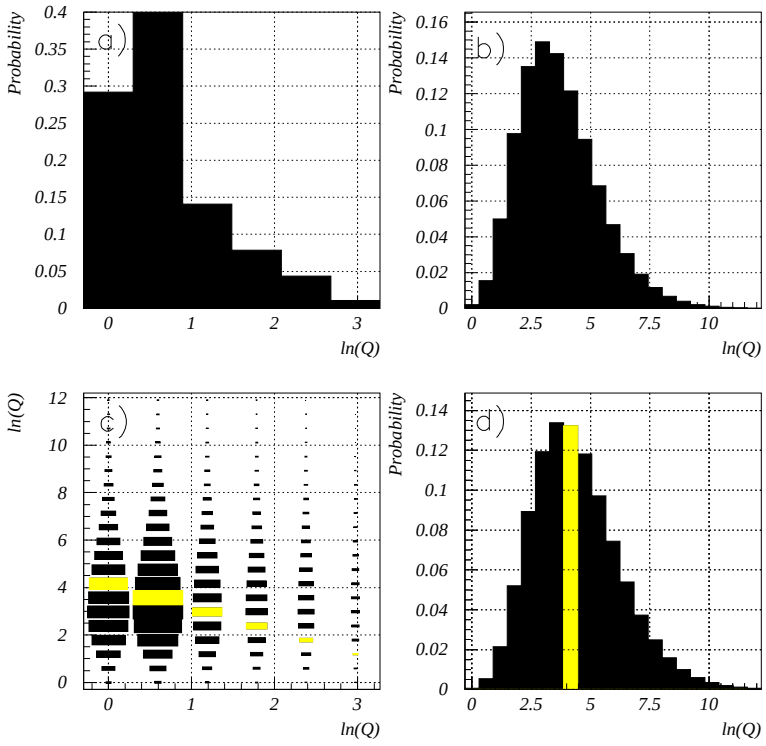

Figure 6.1: How `ALRMC_HIST` uses the different histograms to calculate the p.d.f.'s. The histogram (a) (the histogram for one candidate) is folded with the histogram (b) (the histogram for five candidates) to make the histogram (d) (the histogram for six candidates). The two-dimensional histogram (c) has the histogram for one candidate along the x-axis, and the histogram for five candidates along the y-axis. Each box in the histogram represent the combined probability for that combination. The contributions lying along the light band, *i.e.* the contributions with equal $\ln Q$, are added to get the probability for having a combination with this weight. The $\ln Q$ for one candidate is added to the $\ln Q$ for five candidates to find the $\ln Q$ for six candidates.

While E_CLS and SA_COUNTING simply check whether a new combination already exists, and if it does add the probability for the new combination to the probability for that specific weight, ALRMC_HIST makes a two-dimensional histogram, see Fig. 6.1, with the histogram for one candidate along one axis, and the histogram for the *previous* candidate along the other axis. Then the contributions for different values of $\ln Q$ are found by adding the different entries along the diagonal going from one axis to the other with equal equal $\ln Q$. This two-dimensional histogram is then split along the diagonal, and the contributions lying in the upper half of the diagonal is ignored. This can be done since these contributions are so small they will vanish compared to the other contributions. Estimation of the histogram parameters is done with a few hundred Monte Carlo experiments.

SA_COUNTING estimates the size of the p.d.f. by finding the channel with the largest $\ln Q$, and then multiplying this weight with the number of candidates it will take to have the acummulated Poisson distribution close to unity. Contributions close to this number are ignored, as they will be vanishingly small.

6.2 Comparison of execution speed

To investigate the speed and accuracy of the three different implementations, several analyses of different parts of the mass spectrum in the Higgs search have been made with all three implementations. To illustrate the speed of different implementations, and of the semianalytic method in general, they have been compared to a Monte Carlo routine, ALRMC(Monte Carlo), which is part of the ALRMC package. The calculations were performed on a 2×PentiumII 400 MHz computer running the Linux operating system. The Monte Carlo generations has been done with 100000 Monte Carlo experiments. Table 6.1 shows CPU-time spent in different mass regions of the Higgs search.

mass, step (GeV)	SA_COUNTING	E_CLS	ALRMC_HIST	ALRMC
55.0-95.0, 0.1	1385	1589	786	12475
55.0-65.0, 0.05	861	898	475	7126
85.0-95.0, 0.05	497	634	299	4843

Table 6.1: CPU consumption, in seconds, of the different implementations over different mass hypotheses in the DELPHI Higgs boson search at $\sqrt{s}$=183 GeV.

Comparing the accuracy has been done by calculating the relative differences of the *signal* confidences, $\Delta CL_s/CL_s$, of each of the implementations. Figure 6.2 and 6.3 shows the relative differences.

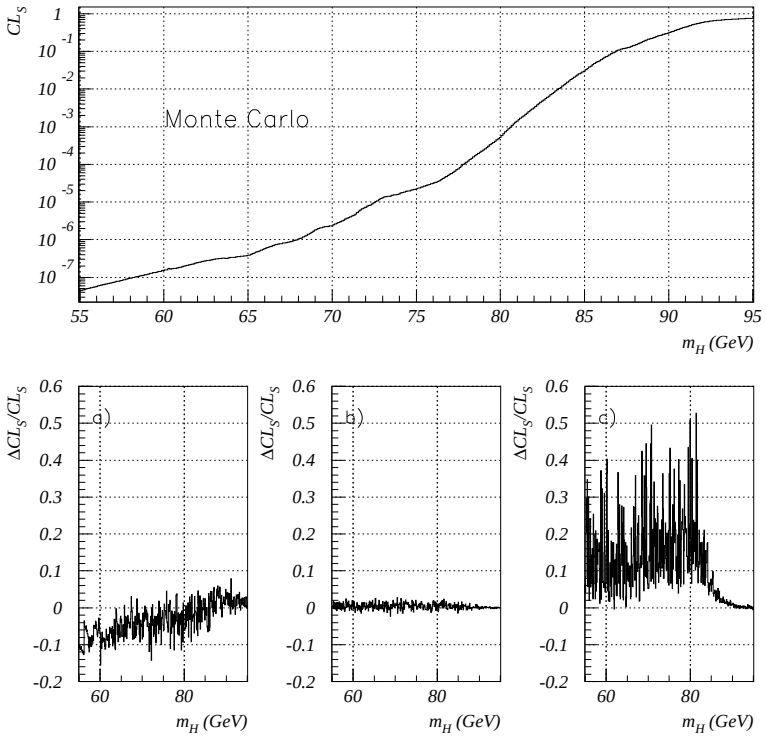

Figure 6.2: The top figure shows the observed CL_s computed by the Monte Carlo routine `ALRMC`(Monte Carlo). The figures (a) through (c) shows the relative differences of the observed CL_s, *i.e.* $\frac{\Delta CL_s}{CL_s}$, calculated by the Monte Carlo routine to, respectively, `SA_COUNTING`, `ALRMC_HIST` and `E_CLS`.

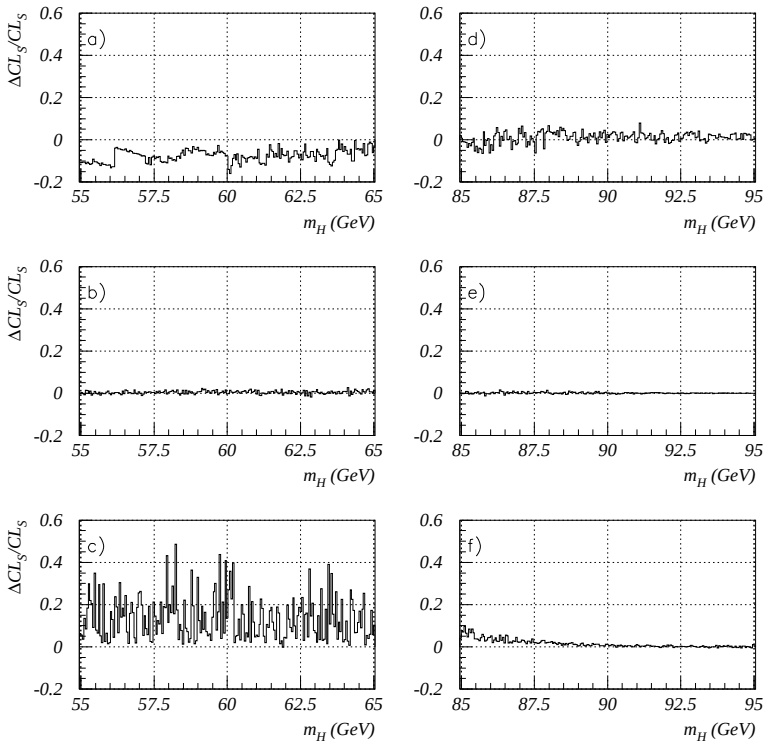

Figure 6.3: Relative difference between the observed CL_S of the three different implementations and `ALRMC`(Monte Carlo). Figure (a) through (c) shows the relative difference between, respectively, `SA_COUNTING`, `ALRMC_HIST` and `E_CLS` in a light Higgs mass-hypotheses region (55 GeV to 65 GeV), while Figure (d) through (f) shows the relative differences in a heavy mass region of the Higgs boson search. Notice how the relative differences converge towards zero as the masses increases.

Notice that the relative differences of all the implementations converges towards zero as the Higgs mass hypotheses increases. This is due to the fact that the programs are tuned to give better results at the heavy Higgs mass hypotheses, where the Higgs hypotheses gives fewer expected signals than the lighter one. This makes the hypotheses of the heavy region both easier and faster to handle than the hypotheses in the light region. In the case of `E_CLS` and `SA_COUNTING`, the heavy Higgs hypotheses gives a shorter list of expected signals and background than the light Higgs hypotheses, for `ALRMC_HIST` the result is a histogram with fewer bins.

6.3 Binning in the different implementations

`E_CLS` has a binning that is part linear and part logarithmic. For probabilities less than 1.0 % the binning is logarithmic, with the default setting being 20 bins per decade. Probabilities larger than 0.01 have a binning that is spaced 0.1 % apart.

`SA_COUNTING` has no predefined bins but makes the bins as the combinations are calculated. This explains in part the disadvantage in speed compared to `ALRMC_HIST`, see Table 6.1. For each new contribution, `SA_COUNTING` has to go through the list of previously calculated combination to see whether or not a new bin has to be added to the list. Determination of the bin size depends on the expected signals and backgrounds. If they have weights with almost the same values, the bins are smaller than if the expected signals and background have fairly different weights.

As default, `ALRMC_HIST` has 2000 bins, which is fewer than both `E_CLS` and `SA_COUNTING`. This is a large part of the explanation of why `ALRMC_HIST` is faster than `E_CLS` and `SA_COUNTING`.

However, both `E_CLS` and `SA_COUNTING` can be changed to have a less fine binning, but the gain in speed will be at the cost of less accuracy.

6.4 Improving the list type implementations

To separate the different channels, `SA_COUNTING` multiplies each channels $\ln Q$ with a number. Since the channels tend to have fairly equal weights, the default is 300. A number smaller than that gives `SA_COUNTING` problems separating the channels, with the result that several channels might end up in the This is a problem that is not dealt with in either of the implementations.

Increasing the number being multiplied to the channels has the effect of increasing number of bins, with increased resolution as the result. As mentioned in the previous section, when increasing the resolution, the CPU consumption also increases, see Figure 6.4 and Table 6.4. When computing the observed CLs with a fine binning, both accuracy and the consistency of the accuracy increases, which can be seen when looking at Figure 6.4.

Factor	CPU consumption (sec)
300	497
500	571
1000	840
1500	1106
2000	1634
2500	1862

Table 6.2: Time spent in CPU loops by `SA_COUNTING` for different values of the number being multiplied to each channels weight.

	`ALRMC`	`ALRMC_HIST`	`E_CLS`	`SA_COUNTING`
m_H (GeV	85.70	85.70	85.65	85.75

Table 6.3: Upper limit of the Higgs mass at 95 % CL using the three different implementations.

6.5 Computed limits

It is clear, when looking at the Figures 6.2 and 6.3 and Table 6.1 that the histogram-type implementation of `ALRMC_HIST` is both faster and more accurate than the list-type implementations of `E_CLS` and `SA_COUNTING`. However, the relative differences between the list-type implementations and the Monte Carlo routine for Higgs mass hypothesis around the upper limit is close to zero and the excluding power of these implementations should be close to `ALRMC_HIST`. When looking at Tab. 6.3, this is proven correct. The different implementations have their upper limit of the Higgs mass at 95 % confidence within 50 MeV of the lower limit computed with the Monte Carlo routine. By increasing the binning, `SA_COUNTING` is able to reproduce the same upper limit as `ALRMC`.

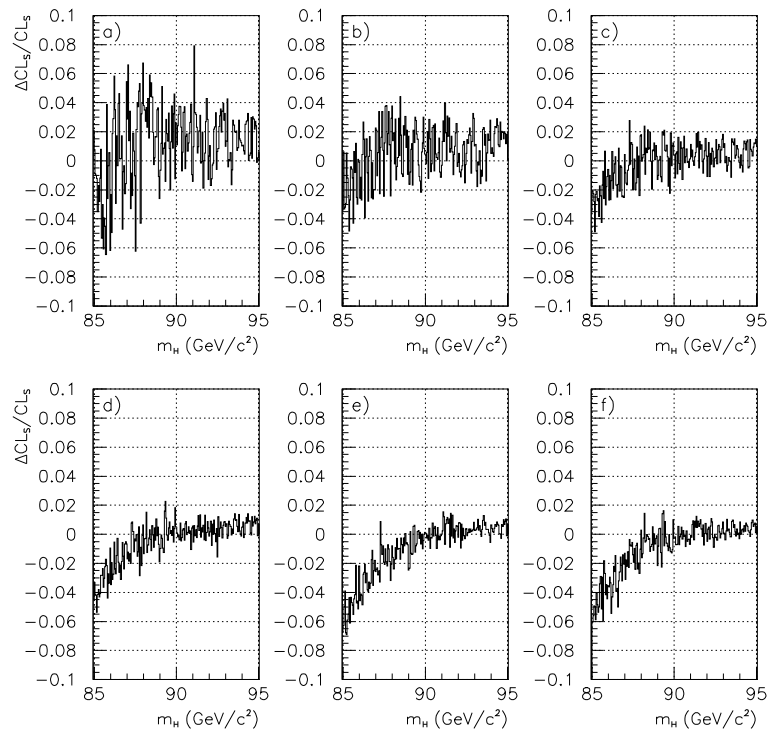

Figure 6.4: The relative difference between `ALRMC` and `SA_COUNTING` for different values of the number multiplied to the weight of each channel, in order to increase the resolution of the binning. Figure (a) through (f) shows observed $\Delta CL_s/CL_s$ when this number is, respectively, 300, which is the default, 500, 1000, 1500, 2000 and 2500.

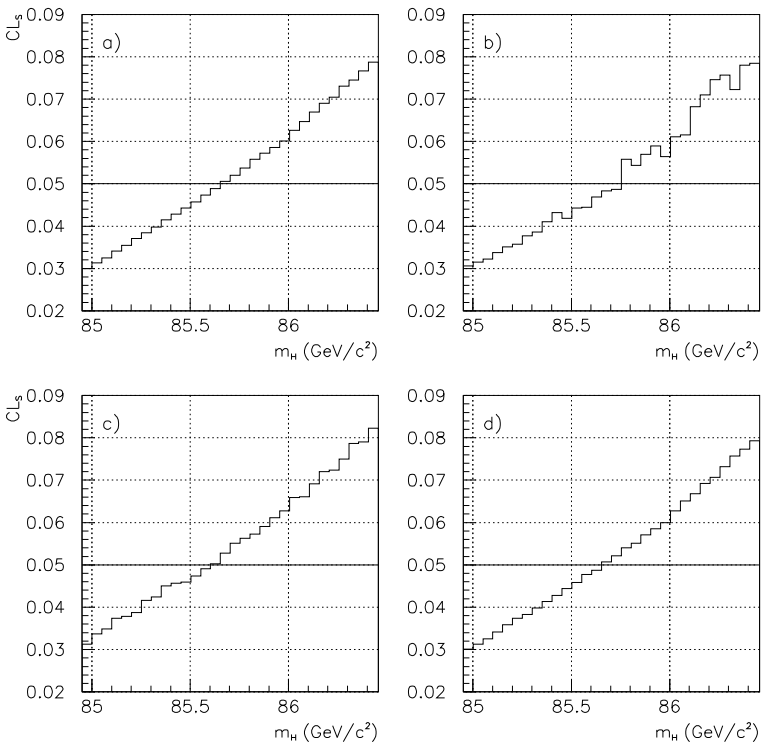

Figure 6.5: Observed confidence limits of the Higgs boson mass calculated with the different implementations, given the 1998 DELPHI data taken at $\sqrt{s}$ GeV.Figure (a) shows the results obtained with `ALRMC`, (b) `SA_COUNTING`, (c) `E_CLS` and (d) `ALRMC_HIST`.

Chapter 7

Search for supersymmetric decay of the W

In [9], a procedure for searches for $W^{\pm}$ bosons decaying into the lightest chargino-neutralino pair,

$$W^{\pm} \rightarrow \tilde{\chi}_1^{\pm} \tilde{\chi}_1^0, \tag{7.1}$$

in W pair production, where one of the W's decays according to the reaction 7.1 and the other to either $q\bar{q}\prime$ or $l\nu_l$, and a method to determine the branching ratio $BR(W \rightarrow \tilde{\chi}_1^{\pm} \tilde{\chi}_1^0)$ is described.

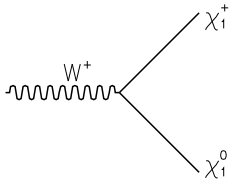

Figure 7.1: The production channel of the lightest positively charged chargino and neutralino.

In models having the sneutrino as the lightest supersymmetric particle (LSP), the chargino of Eq. 7.1 will, if its mass is slightly above the LSP mass, decay into a sneutrino and a charged lepton:

$$\tilde{\chi}_1^+ \rightarrow \tilde{\nu}_l l^+. \tag{7.2}$$

Only the positively charged reactions are shown, the charge conjugated reactions are left out for convenience; they are just as likely to happen. If the SM decaying W decays hadronically, the detection of the sparticles is almost impossible if the mass difference of the chargino and the sneutrino, $\Delta M = m_{\tilde{\chi}_1^+} - m_{\tilde{\nu}}$, are below a few GeV. The sneutrino-lepton pair of Eq. 7.2

will be soft, and hidden inside the total event. On the other hand, if the SM decaying W decays into a lepton-neutrino pair, the low event multiplicity can make the detection of the supersymmetric particles possible. The experimental signature can thus be said to be hard leptons plus missing energy. In the analysis described in [9], the selection cuts have been split into two, one for ΔM between 0 GeV and 0.5 GeV and one for $< \Delta M$ between 0.5 GeV and 2 GeV.

In the analysis described in [9], the confidence limit of the branching ratio of the reaction described above has been calculated with the simple "PDG method", *i.e.* that all information has been put into one bin. The analysis has been reproduced to see the advantages of using a more sophisticated method of computing the confidence limits, such as `SA_COUNTING`, compared to the simple method used in [9].

7.1 Event selection

During the 1997 runs at LEP, with center-of-mass energy $\sqrt{s} \simeq 183$ GeV, 54 pb^{-1} of data was collected at the DELPHI detector. 51.65 pb^{-1} of this collection has been declared suitable for data analysis (the rest have been left out due to some problem or inefficiency in the detectors). Of the data collected at the 172 GeV run in 1996, 9.98 pb^{-1} is used.

The different event selections and cuts are described in detail in [9], pp. 2-10. Several Monte Carlo generators were used to create simulated events, which in turn gave rise to the criteria used in selection of the experimental events.

Shower selection

Some of the criteria deciding whether a charged track can be used or not, given by the shower selection, are

- $|\vec{p}| > 200$ MeV,
- Track length has to be over 20 cm, unless it's a VD-only (see Fig. 3.2) track. In that case it has to stay outside $\pm 3^o$ of the 90^o.

Rescaling of the track momentum is attempted if, for more than six charged tracks, the track momentum is greater than 75 % of the beam momentum, or in the case of zero to six charged events the track momentum is greater than 125 % of the beam momentum. Unassociated showers in the calorimeters are accepted if their energy is above 0.5 GeV (or above 0.75 GeV if the shower is in the HAC).

Tracks not meeting these requirements does not enter the calculations for the overall event properties, but they are kept as *locked* tracks.

Preselection

For tracks with more than six charged particles in the shower, they have to have

- $40 < E_{vis} < 120$ GeV,
- $E_{trans} > 20$ GeV,
- Missing $p_{trans} > 15$ GeV,
- The demand on the polar angle of the thrust is $\vartheta_{thr} 30^o < \vartheta_{thr} < 50^o$.

Tracks with a charged multiplicity between zero and six have to meet:

- $E_{visible} > 10$ GeV,
- The energy fraction carried by the hardest particle must be more than 80 % of the visible energy. The energy fraction carried by the most energetic jet has to be above 90 % of the visible energy,
- If the charged multiplicity is above one, then $30^o < \vartheta_{thr} < 150^o$.

If a track has passed the preselection, the following cuts are applied:

Selection of hadronic showers

In showers with more than six charged tracks, the tracks are accepted if

- the visible energy is above 90 GeV,
- invariant mass of all particles is between 55 GeV and 85 GeV,
- there are no identified electrons or muons with energy above 5 GeV,
- no isolated charged particle is detected with energy above 15 GeV.

Selection of leptonic showers

The selection of leptonic tracks are divided in one in the case of ΔM very small, 0 GeV $< \Delta M <$ 0.5 GeV, and one in the case of ΔM small, 0.5 GeV $< \Delta M <$ 2.0 GeV. If ΔM is very small, the selection cuts on leptonic tracks are

- Number of charged particles has to be one, two or three,
- Visible energy less than 80 GeV,
- Energy of the hardest track for $\sqrt{s}$=183 GeV data between 24 GeV and 74 GeV and for $\sqrt{s}$=172 GeV data between 26 and 62 GeV,

- No neutral shower with energy above 5 GeV is allowed,
- No *locked* tracks with energy above 3 GeV.

For small ΔM, the cuts are much the same, but the demand on the *locked* tracks is that they cannot have energy above 5 GeV, and the charged multiplicity must be exactly two.

7.2 Predicted backgrounds and signals

The predicted signal efficiencies found by Monte Carlo simulations are listed in Table 7.1 and the expected background rates are listed in Table 7.3 and 7.2.

	Δ M = 0 GeV	Δ M = 0.5 GeV	Δ M = 2 GeV
HADRONIC CHANNEL (183 GeV)			
	0.159		
LEPTONIC CHANNEL (183 GeV)			
selection A	0.131	0.121	
selection B		0.104	0.110
HADRONIC CHANNEL (172 GeV)			
	0.166		
LEPTONIC CHANNEL (172 GeV)			
selection A	0.111	0.118	
selection B		0.106	0.104

Table 7.1: Efficiencies for selecting $\tilde{\nu} l^+$ decaying from χ^+. The χ^+ is a decay product of the reaction $W^+W^- \to \tilde{\chi_1}^+ \tilde{\chi_1}^0$. Selection A and B refer to the selections optimized to $0 < \Delta M < 0.5$ GeV and 0.5 GeV $< \Delta M <$ 2 GeV, respectively.

	Hadronic selection	Leptonic selection ($0 < \Delta M < 0.5$)	Leptonic selection ($0.5 < \Delta M < 2$)
Σ pred. bg. rates	8.89	5.02	2.57
Observed events	8	4	2

Table 7.2: The Standard Model predicted backgrounds and observed candidates remaining after the cuts from the $\sqrt{s}$=183 GeV run at LEP200.

Of the backround processes, $e^+e^- \to Z^0(n\gamma) \to \tau^+\tau^-(n\gamma)$ and $e^+e^- \to l\nu_l l'\nu_{l'}$ are the main background processes in the leptonic sector with 0.5<

	Hadronic selection	Leptonic selection ($0 < \Delta M < 0.5$)	Leptonic selection ($0.5 < \Delta M < 2$)
Σ predicted background	1.85	0.93	0.37
Observed events	2	0	0

Table 7.3: The Standard Model predicted backgrounds and observed candidates left after the cuts from the $\sqrt{s}$=172 GeV run at LEP200.

$\Delta M < 2$ GeV, Bhabha and Compton scattering and $e^+e^- \to l\nu_l l\prime\nu_{l\prime}$ processes dominate in the leptonic sector with $0 < \Delta M < 0.5$ GeV. In the hadronic sector the processes $e^+e^- \to \tau\nu_\tau q\bar{q}l\prime$, $e^+e^- \to l\nu_l l\prime\nu_{l\prime}$ and $e^+e^- \to Z^0(n\gamma) \to q\bar{q}(n\gamma)$ dominate the background.

7.3 Computing limits on the branching ratios using SA_COUNTING

The expected signal and background rates found in Tables 7.1, 7.3 and 7.2 include, due to limited Monte Carlo statistics, uncertainties (these are shown in [9]). Since SA_COUNTING (see Appendix A) does not handle uncertainties, these errors have not been included in the calculations.

Table 7.1 shows the efficiencies of selecting $e^+e^- \to W^+W^-$ events with one W decaying supersymmetricly according to Eq. 7.1 and the other decaying into Standard Model particles. However, when calculating the branching ratio, it is the expected signal ratio that is used. This quantity can be found by defining the fraction of W decaying into chargino-neutralino pairs as

$$x = BR(W^\pm \to \tilde{\chi}_1^\pm \tilde{\chi}_1^0). \tag{7.3}$$

This means that the fraction of processes decaying into standard model particles only is $(1-x)$. The branching ratio of W^+W^- where one W decays into SUSY particles and the other into SM particles thus has a fraction of $2x(1-x)$. The number of expected events N is then found by

$$N = 2x(1-x) \sum_{E_{cms}} \mathcal{L}_i \sigma_i^{th} \varepsilon_i, \tag{7.4}$$

where the sum is over the different center-of-mass energies, $\mathcal{L}_i$ are the different luminosities, recall that the luminosity for the $\sqrt{s}$=183 GeV run is 51.65 pb^{-1} and 9,98 pb^{-1} for the 172 GeV data. σ_i^{th} are the theoretical cross-section of W's decaying into a chargino-neutralino pair and ε_i are the detector efficiencies. The *measured* cross-section only takes SM decays into account, since there is no experimental evidence of the existence of SUSY

particles. An expression for supersymmetric cross-section given the measured cross-section, is given by

$$\sigma^{th} = \frac{\sigma^{meas}}{(1-x)^2}. \tag{7.5}$$

Using this expression for the cross-section, the number of expected events is

$$N = \frac{2x}{(1-x)} \sum_{E_{cms}} \mathcal{L}_i \sigma_i^{meas} \varepsilon_i. \tag{7.6}$$

The branching ratio at a 95 % confidence limit is then found by calculating the confidence of the expected signal and background rates, using the program `SA_COUNTING`, for different values of the fraction x.

	ΔM=0 GeV	ΔM=0.5 Gev	ΔM=2 GeV
183 GeV	1.50 %	1.56 %	1.40 %
172 GeV	6.08 %	6.34 %	6.39 %
Combined	1.34 %	0.99 %	1.32 %

Table 7.4: The *observed* branching ratio at 95 % confidence, using `SA_COUNTING`, for 172 and 183 GeV. The column 'Combined' is the results obtained when the data for the two different center-of-mass energies are combined. The largest branching ratio in the 'combined' column is taken to be the branching ratio.

	ΔM=0 GeV	ΔM=0.5 GeV	ΔM=2 GeV
183 GeV	2.16 %	2.24 %	2.05 %
172 GeV	8.32 %	7.65 %	7.71 %
Combined	2.11 %	1.61 %	1.94 %

Table 7.5: The *expected* branching ratio at 95 % confidence, using `SA_COUNTING`, for 172 and 183 GeV.

Taking the worst, *i.e.* the largest, result in the column 'Combined' in Table 7.4 as the branching ratio, the *observed* branching ratio at 95 % CL is found to be

$$BR_{obs}(W^{\pm} \to \tilde{\chi}_1^{\pm} \tilde{\chi}_1^0) < 1.34\%. \tag{7.7}$$

In the same manner, looking at Table 7.5 the *expected* branching ratio is found to be

$$BR_{expect}(W^{\pm} \to \tilde{\chi}_1^{\pm} \tilde{\chi}_1^0) < 2.11\%. \tag{7.8}$$

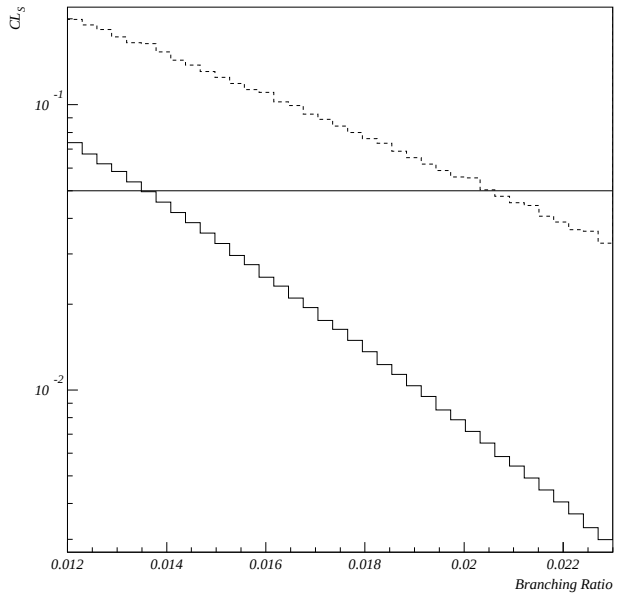

Figure 7.2: The combined results for ΔM=0 GeV, which is the value of Δ M that yields the largest branching ratios. The solid line is the observed branching ratio, the dashed line is the expected ratio

The observed branching ratio is slightly smaller than the expected ratio, which means that there are fewer background events than what had been expected. With the definition of the hypothesis saying that there are no supersymmetric decays of the W as the *null* hypothesis, one can say that this hypothesis has been excluded stronger than what had been expected.

If these branching ratios had been computed using the simple PDG method, instead of the method described in Chapter 6, the *observed* branching ratio would have been 1.54 % and the *expected* branching ratio would have been 2.17 %.

The calculated observed branching rate of [9], is 1.56% which is in good agreement with the result obtained using the PDG method (the analysis of [9] does not include calculations of the expected branching ratio). Comparing the results obtained using `SA_COUNTING` with the results obtained using the simple PDG method, it is clear that the semianalytic method is the stronger of the two, although the difference is fairly small. Table 7.2 shows that in this search, the hadronic channel dominated the other channels. This makes the differences between the semianalytical and the PDG method smaller. Had the observed candidates and expected signal and background rates been more evenly distributed among the channels, the differences between the two methods would have been increased.

In the calculations for the branching ratios, the assumption that $BR(\tilde{\chi}_1^{\pm} \rightarrow$

$\tilde{\nu}_l l^{\pm}) \simeq 1$ has been made.

7.4 MSSM parameter exclusion

Having found an upper limit on the *observed* branching ratio, one can use Eq. 2.47,

$$\Gamma(W^+ \to \chi_i^+ \chi_j^0) = \frac{G_F m_W^3 \lambda_{ij}^{1/2}}{6\sqrt{2}\pi}$$
$$\times\{[2 - \kappa_i^2 - \kappa_j^2 - (\kappa_i^2 - \kappa_j^2)^2](Q_{Lij}^2 + Q_{Rij}^2)$$
$$+12\kappa_i\kappa_j Q_{Lij} Q_{Rij}\},$$

where the matrices Q_{Rij} and Q_{Lij} are linear combinations of the diagonalized gaugino mixing matrices, recall Eq. 2.49, and instead of summing over all the different charginos and neutralinos, the equation is solved for the lightest chargino-neutralino pair, which is equal to setting i and j equal to one. The regions in the parameter space of the higgsino and bino masses that are excluded at the same confidence limit as the branching ratio, *i.e.* at 95 % CL, can then be found.

The partial width for $W^{\pm}$ decaying into a chargino-neutralino pair is given by

$$\Gamma(W^{\pm} \to \tilde{\chi}_1^{\pm} \tilde{\chi}_1^0) = BR(W^{\pm} \to \tilde{\chi}_1^{\pm} \tilde{\chi}_1^0) \cdot \Gamma(W^{\pm} \to anything), \qquad (7.9)$$

and since both the total width of the W, $\Gamma(W^{\pm} \to anything)$ and the branching ratio, $BR(W^{\pm} \to \tilde{\chi}_1^{\pm} \tilde{\chi}_1^0)$ is known, the partial width is given.

The neutralino and chargino masses are found when the charged and neutral gaugino mass-matrices, see Eq 2.32 and 2.44, are diagonalized, but the masses of the gauginos and the higgsino are parameters not decided by the theory. By varying the bino and the higgsino masses, expressions for the chargino and neutralino masses can be found.

The Higgs mixing term $\tan\beta$ have been fixed, and M_2 and μ have been varied to find the regions of the (M_2, μ) parameter space that are allowed. In Fig. 7.3 and Fig. 7.4 the regions with allowed higgsino and bino masses are found for several values of $\tan\beta$.

Compared with the excluded regions of the (M_2, μ) plane for different values of $\tan\beta$ of Ref. [9], the improved branching ratio results in a slightly increase of the excluded regions, see Figure 7.5.

The computations have been performed using `SUSYPAR`, see Appendix B.

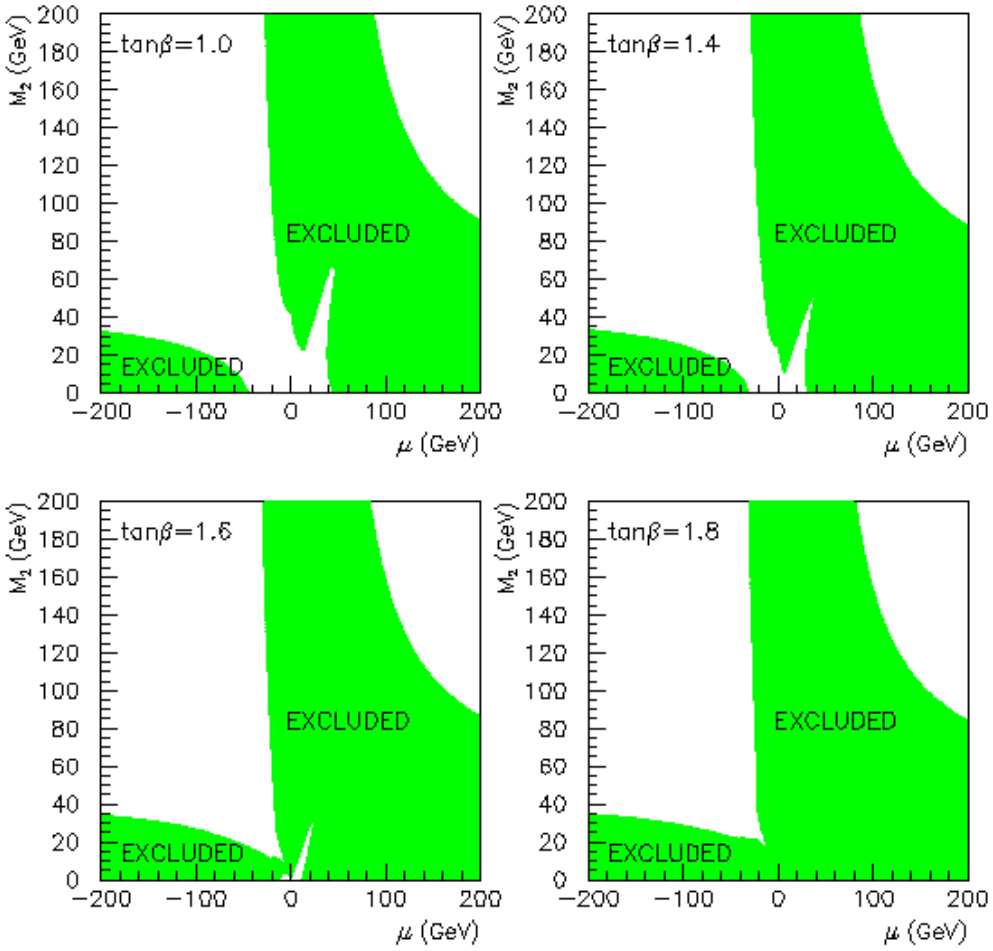

Figure 7.3: The excluded regions in the (M_2, μ) plane for small values of $\tan\beta$. Notice how the two excluded regions at $\tan\beta$=1.0 merge into one as $\tan\beta$ increases.

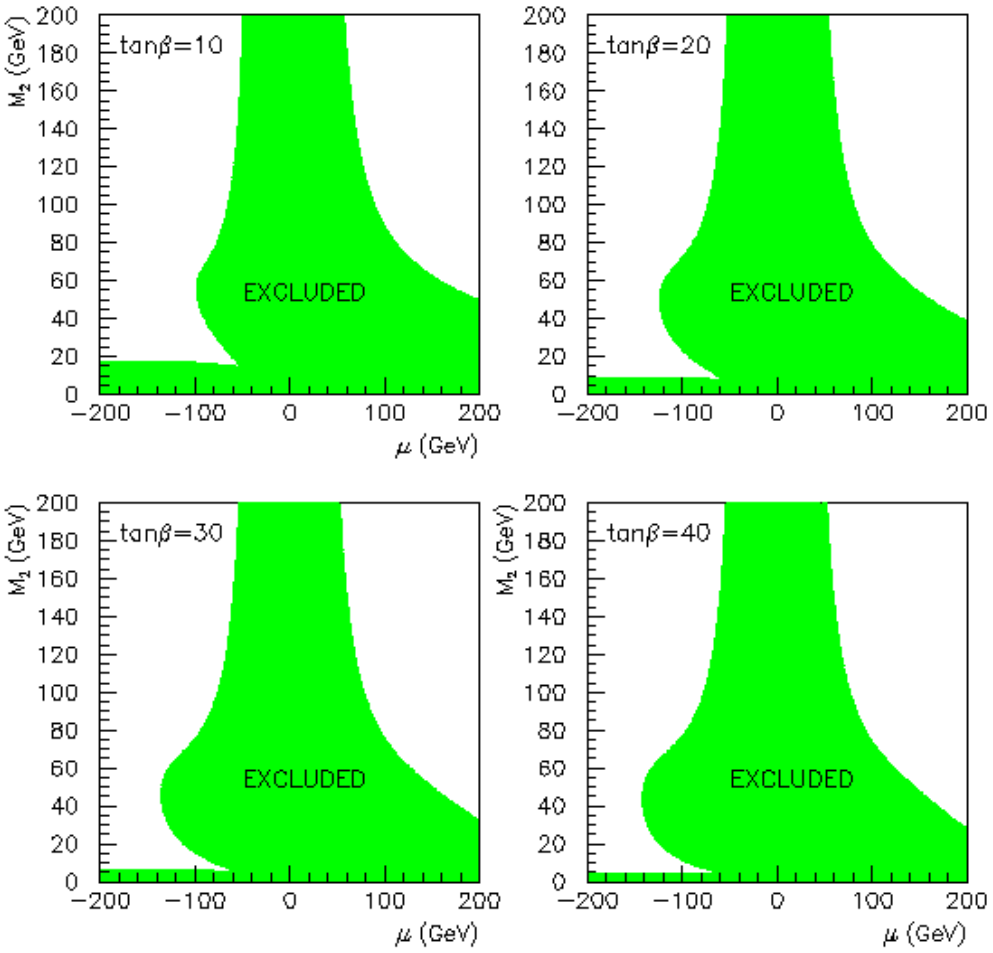

Figure 7.4: The excluded regions of the (M_2, μ) plane for larger values of $\tan\beta$. The onion-shape of the excluded region grows as the value of $\tan\beta$ increases.

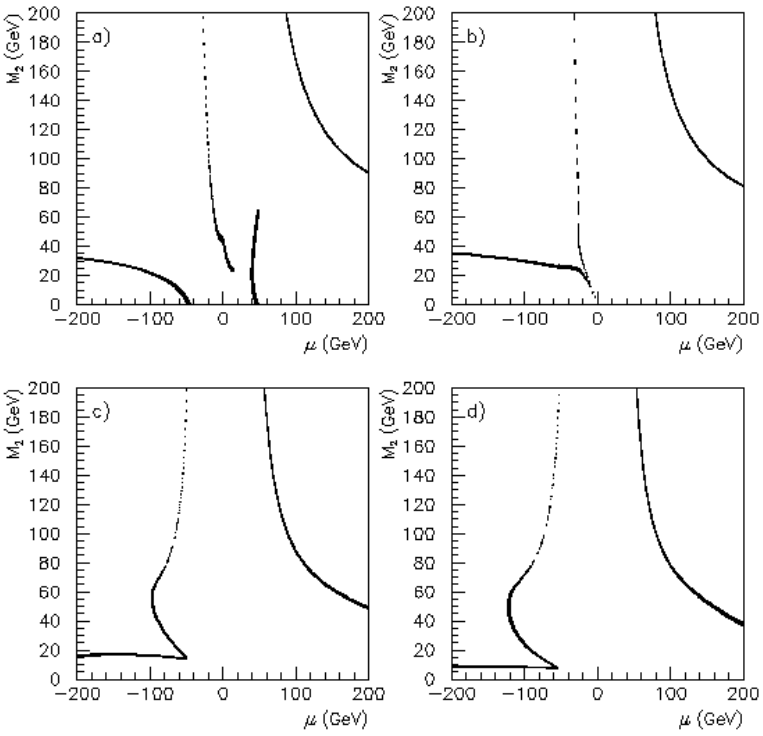

Figure 7.5: The difference between the (M_2, μ) planes excluded using the branching ratio obtained with the semianalytical method and the branching ratio obtained using the PDG method for (a) tan β=1.0, (b) tan β=2.0, (c) tan β=10.0 and (d) tan β=20.0.The difference between the planes calculated with the two branching ratios are lying along the edge of the excluded regions.

Chapter 8

Conclusions and outlook

8.1 Physics results

As is seen in Chapter 5 no trace of the existence of a Higgs boson is seen up to a center-of-mass energy of 183 GeV. This corresponds to the exclusion at a 95 % confidence level of a Higgs boson with mass less than 85.7 GeV.

In Chapter 6 it was shown that if the W boson decays into a pair of supersymmetric particles, the branching ratio of this process is less than 0.0134.

- $\mathrm{BR}(W^{\pm} \to \tilde{\chi}_1^{\pm}\tilde{\chi}_1^0) < 1.34\%$ (95% CL)

With this branching ratio, one can exclude part of the SUSY parameter space, in this case the chosen space was the mass of the higgsino and bino.

The essence of this is that at the energies these two searches have been performed, there are no traces of new physics.

8.2 Technical results and outlook

Implementating and developing the semianalytic confidence limit calculator `SA_COUNTING`, proved that when used in a search with many channels, as the Higgs boson search, the list type implementations was both slower and more unprecise than what had been hoped for.

Given more time, I would like to understand the handling of systematic uncertainties. In Ref. [20], Cousins and Highland describe a method to incorporate statistical uncertainties in one-channel searches. This can be generalized into searches with several distinct channels, see for example Ref. [21].

I am pretty sure there must be a less CPU-consuming method of handling the list, but this is evidently not as intuitive as the one implemented in `SA_COUNTING`, and it would had been exciting to see if a smarter implementation could have been developed.

I was also told near the end of my work with this thesis that another, even faster method of computing the likelihood ratio probability density functions has been developed which is based on Fourier transforming the channels, and it would be interesting to understand this method.

Appendix A

```
      PROGRAM sa_counting_v2
*
*....Program that calculates the probability distribution functions
*....(p.d.f.) of hypothesis semianalytical, with the use of the likelihood
*....ratio test-statistic
*
      IMPLICIT NONE

      INTEGER nchan,no_bins
      REAL sa_counting,ppois,t

      COMMON/params/nchan,no_bins
      EXTERNAL sa_counting

*
*....reading the number of search channels and number of bins in the
*....p.d.f-list from file param.h
*
      OPEN(10,name='param.h',status='old')
      READ(10,100)nchan
      READ(10,101)no_bins
 100  FORMAT(I2)
 101  FORMAT(I5)
      CLOSE(10)

*
*....calling the main routine
*
      CALL saco_v2

      END
*******************************************
*......This is just a trick to allow dynamic
```

```
*......memory allocation of the long arrays
************************************************

      SUBROUTINE saco_v2
      IMPLICIT NONE

*
*....variables
*
*....Number of channels and number of bins
*
      INTEGER nchan,no_bins
      COMMON/params/nchan,no_bins

*....counting variables
      INTEGER i,j,k,l,m,n
      INTEGER k_sb,m_sb
      INTEGER next_length,nl_sb !the length of the p.d.f-arrays
      INTEGER n_o(nchan)

*
*....Variables concerning the total integrated signal and background rates
*....and Poisson probabilities
*
      REAL wt(nchan),b(nchan),s(nchan),pwtsb(nchan)
      REAL pwtb(nchan),stot,btot,ptotb,ptotsb,wb,wsb

      REAL itemp1b,itemp2b
      REAL itemp1sb,itemp2sb

*
*....These variables concerns the arrays the p.d.f.'s are made from
*....one_b and one_sb are the arrays for the integrated b and (s+b)
*....rates, resp. next_b and next_sb is the arrays for the p.d.f.'s
*....for (n-1) candidates that has NOT been multiplied with the approprialte
*....Poisson-prob. result_b & result_sb are the arrays for the accumulated p.d.f's
*
      REAL one_b(2,nchan),next_b(2,no_bins),new_b(2,no_bins)
      REAL result_b(2,no_bins),integr_b(no_bins)
      REAL cl_b,cl_s

      REAL one_sb(2,no_bins),next_sb(2,no_bins)
      REAL new_sb(2,no_bins),result_sb(2,no_bins)
      REAL integr_sb(no_bins),cl_sb
```

```
      REAL expt,wt_expt,gen_xisq

*
*....the expected confidences
*
      REAL interm_s(no_bins),cl_s_infty
      REAL interm_sb(no_bins),cl_sb_infty

      REAL ppois
      EXTERNAL ppois

*
*....HBOOK stuff
*
      integer mwp,h
      parameter(mwp=10000)
      common/pawc/h(mwp)
      real itemp1,itemp2
      real t


      DO i=1,no_bins
         next_b(1,i)=0.
         new_b(1,i)=0.
         result_b(1,i)=0.
      ENDDO

      DO i=1,no_bins
         next_sb(2,i)=0.
         new_sb(2,i)=0.
         result_sb(2,i)=0.
      ENDDO


*
*....Reading the integrated signal and background rates and number of
*....observed candidates from file date.19
*
      OPEN(10,name='data.19',status='old')
      DO i=1,nchan
         READ(10,*)s(i),b(i),n_o(i)
      ENDDO
```

```
 100  FORMAT(F6.4,T9,F6.4,T17,I2)
      CLOSE(10)

      ptotb=0.
      ptotsb=0.
      btot=0.
      stot=0.
      expt=0.

*
*....initial calculations. wt(i) = the weigth of channel #i
*....expt = the observed value
*
     DO i=1,nchan
         wt(i)=ALOG(1.+s(i)/b(i))
         pwtb(i)=b(i)
         pwtsb(i)=s(i)+b(i)
         ptotb=ptotb+pwtb(i)
         ptotsb=ptotsb+pwtsb(i)
         stot=stot+s(i)
         btot=btot+b(i)
         expt=expt+n_o(i)*(1+INT(500*wt(i)))
         wt_expt=wt_expt+(n_o(i)*wt(i))
      ENDDO

      DO i=1,nchan
         pwtb(i)=pwtb(i)/ptotb
         pwtsb(i)=pwtsb(i)/ptotsb
      ENDDO

*
*....Initializing the list of int. sign. and bg. rates
*
      DO i=1,nchan
         one_b(1,i)=1.+INT(500*wt(i))
         one_b(2,i)=pwtb(i)
         one_sb(1,i)=1.+INT(500*wt(i))
         one_sb(2,i)=pwtsb(i)
      ENDDO


*
*....Chek to see if to channels end up in the same bin
*....If this happens, no one knows exactly what will happen!
```

```
*
      DO i=1,nchan
         DO j=1,i-1
            IF(one_b(1,i).EQ.one_b(1,j))THEN
               PRINT *,'>>>>>>>'
               PRINT *,'>>>>>>>TWO CHANNELS IN SAME BIN'
               PRINT *,'>>>>>>>SOMEWHAT UNRELIABLE RESULTS'
               PRINT *,'>>>>>>>'
            ENDIF
         ENDDO
      ENDDO

*
*....Preparing the histograms for one candidate
*
      wb=ppois(btot,1)
      wsb=ppois(stot+btot,1)

      DO i=1,nchan
         next_b(1,i)=one_b(1,i)
         next_b(2,i)=one_b(2,i)
         next_sb(1,i)=one_sb(1,i)
         next_sb(2,i)=one_sb(2,i)
      ENDDO



*
*....Making the one candidate-histograms
*
      DO i=1,nchan
         result_b(1,i)=one_b(1,i)
         result_b(2,i)=one_b(2,i)*wb
         result_sb(1,i)=one_sb(1,i)
         result_sb(2,i)=one_sb(2,i)*wsb
      ENDDO

*
*....Histogram for two candidates, background only
*

*....This is the final two candidates histogram, multiplied with
*....the Poissonprobability
```

```
*
      k=1
      m=nchan+1
      wb=ppois(btot,2)
      DO i=1,nchan
         DO j=1,nchan
            itemp1b=one_b(1,i)+one_b(1,j)
            itemp2b=one_b(2,i)*one_b(2,j)
            DO l=1,m-1
               IF(ABS(result_b(1,l)-itemp1b).LT.1.5)THEN
                  result_b(2,l)=result_b(2,l)+itemp2b*wb
                  GOTO 197
               ENDIF
            ENDDO
            result_b(1,m)=itemp1b
            result_b(2,m)=itemp2b*wb
            m=m+1
 197        CONTINUE
         ENDDO
      ENDDO

*
*....This is just an 'intermediary' working vector for two candidates
*....(actually, it's identical to the result-vector, but it isn't
*....multiplied with the Poissonprobability)
*

      DO i=1,nchan
         DO j=1,nchan
            itemp1b=one_b(1,i)+one_b(1,j)
            itemp2b=one_b(2,i)*one_b(2,j)
            DO l=1,k-1
               IF(ABS(next_b(1,l)-itemp1b).LT.1.5)THEN
                  next_b(2,l)=next_b(2,l)+itemp2b
                  GOTO 198
               ENDIF
            ENDDO
            next_b(1,k)=itemp1b
            next_b(2,k)=itemp2b
            k=k+1
 198        CONTINUE
         ENDDO
      ENDDO
```

```
*
*....Histograms for two candidates, this time for signal+background
*....Same story as the background only-histogram
*

      k_sb=1
      m_sb=nchan+1
      wsb=ppois(stot+btot,2)
      DO i=1,nchan
         DO j=1,nchan
            itemp1sb=one_sb(1,i)+one_sb(1,j)
            itemp2sb=one_sb(2,i)*one_sb(2,j)
            DO l=1,m_sb-1
               IF(ABS(result_sb(1,l)-itemp1sb).LT.1.5)THEN
                  result_sb(2,l)=result_sb(2,l)+itemp2sb*wsb
                  GOTO 200
               ENDIF
            ENDDO
            result_sb(1,m_sb)=itemp1sb
            result_sb(2,m_sb)=itemp2sb*wsb
            m_sb=m_sb+1
 200        CONTINUE
         ENDDO
      ENDDO

      DO i=1,nchan
         DO j=1,nchan
            itemp1sb=one_sb(1,i)+one_sb(1,j)
            itemp2sb=one_sb(2,i)*one_sb(2,j)
            DO l=1,k_sb-1
               IF(ABS(next_sb(1,l)-itemp1sb).LT.1.5)THEN
                  next_sb(2,l)=next_sb(2,l)+itemp2sb
                  GOTO 201
 3             ENDIF
            ENDDO
            next_sb(1,k_sb)=itemp1sb
            next_sb(2,k_sb)=itemp2sb
            k_sb=k_sb+1
 201        CONTINUE
         ENDDO
      ENDDO

*
*....Folding for the rest of the candidates. Folding until the
```

```
*....background prob. is nearly 1.0
*
      ptotb=ppois(btot,0)+ppois(btot,1)+wb
      n=2
      next_length=k-1
      nl_sb=k_sb-1
      DO WHILE(ptotb.LT.0.999)  !OBS 0.999999
         n=n+1
         wb=ppois(btot,n)
         wsb=ppois(stot+btot,n)
         ptotb=ptotb+wb
         k=1
         k_sb=1
         DO i=1,nchan
            DO j=1,next_length
               itemp1b=one_b(1,i)+next_b(1,j)
               itemp2b=one_b(2,i)*next_b(2,j)
               DO l=1,k-1
                  IF(ABS(new_b(1,l)-itemp1b).LT.1.5)THEN
                     new_b(2,l)=new_b(2,l)+itemp2b
                     GOTO 399
                  ENDIF
               ENDDO
               new_b(1,k)=itemp1b
               new_b(2,k)=itemp2b
               k=k+1
 399           CONTINUE
            ENDDO
         ENDDO
         next_length=k-1
         DO i=1,next_length
            next_b(1,i)=new_b(1,i)
            next_b(2,i)=new_b(2,i)
         ENDDO
         DO i=1,nchan
            DO j=1,nl_sb
               itemp1sb=one_sb(1,i)+next_sb(1,j)
               itemp2sb=one_sb(2,i)*next_sb(2,j)
               DO l=1,k_sb-1
                  IF(ABS(new_sb(1,l)-itemp1sb).LT.1.5)THEN
                     new_sb(2,l)=new_sb(2,l)+itemp2sb
                     GOTO 499
                  ENDIF
               ENDDO
```

```
               new_sb(1,k_sb)=itemp1sb
               new_sb(2,k_sb)=itemp2sb
               k_sb=k_sb+1
 499           CONTINUE
            ENDDO
         ENDDO
         nl_sb=k_sb-1
         DO i=1,nl_sb
            next_sb(1,i)=new_sb(1,i)
            next_sb(2,i)=new_sb(2,i)
         ENDDO
         DO i=1,next_length
            itemp1b=next_b(1,i)
            itemp2b=next_b(2,i)
            DO j=1,m-1
               IF(ABS(result_b(1,j)-itemp1b).LT.1.5)THEN
                  result_b(2,j)=result_b(2,j)+itemp2b*wb
                  GOTO 599
               ENDIF
            ENDDO
            result_b(1,m)=itemp1b
            result_b(2,m)=itemp2b*wb
            m=m+1
 599        CONTINUE
         ENDDO
         DO i=1,nl_sb
            itemp1sb=next_sb(1,i)
            itemp2sb=next_sb(2,i)
            DO j=1,m_sb-1
               IF(ABS(result_sb(1,j)-itemp1sb).LT.1.5)THEN
                  result_sb(2,j)=result_sb(2,j)+itemp2sb*wsb
                  GOTO 699
               ENDIF
            ENDDO
            result_sb(1,m_sb)=itemp1sb
            result_sb(2,m_sb)=itemp2sb*wsb
            m_sb=m_sb+1
 699        CONTINUE
         ENDDO
      ENDDO


*
*....Inserting the zero candidates-histogram into the result-vector
```

```
*....by hand
*
      result_b(1,m)=0.
      result_b(2,m)=EXP(-btot)
      result_sb(1,m_sb)=0.
      result_sb(2,m_sb)=EXP(-stot-btot)

*
*....sorting the result-vector (background only) with respect to
*....the weigths
*
      DO i=1,m
         DO j=1,i-1
            IF(result_b(1,j).GT.result_b(1,i).AND.result_b(2,i)
     &.NE.0.0)THEN
               itemp1=result_b(1,i)
               itemp2=result_b(2,i)
               result_b(1,i)=result_b(1,j)
               result_b(2,i)=result_b(2,j)
               result_b(1,j)=itemp1
               result_b(2,j)=itemp2
            ENDIF
         ENDDO
      ENDDO

*
*....Sorting the result-vector (signal+background)
*
      DO i=1,m_sb
         DO j=1,i-1
            IF(result_sb(1,j).GT.result_sb(1,i).AND.result_sb(2,i)
     &.NE.0.0)THEN
               itemp1=result_sb(1,i)
               itemp2=result_sb(2,i)
               result_sb(1,i)=result_sb(1,j)
               result_sb(2,i)=result_sb(2,j)
               result_sb(1,j)=itemp1
               result_sb(2,j)=itemp2
            ENDIF
         ENDDO
      ENDDO

*
*....Writing the y-coordinates of the p.d.f's in ascending order
```

```
*....to file p_pdf and sb_pdf
*
      open(19,name='b_pdf',status='unknown')
      open(20,name='sb_pdf',status='unknown')
      do i=1,m
         write(19,*)result_b(2,i)
      enddo

      do i=1,m_sb
         write(20,*)result_sb(2,i)
      enddo
      close(19)
      close(20)

*
*....Preparing the integration of both the bg. only and the s+b
*....vectors
*
      DO i=1,no_bins
         integr_b(i)=result_b(2,i)
         integr_sb(i)=result_sb(2,i)
       ENDDO

*
*....Integrating!
*
      DO i=2,no_bins
         integr_b(i)=integr_b(i)+integr_b(i-1)
         integr_sb(i)=integr_sb(i)+integr_sb(i-1)
      ENDDO



*
*....Writing the integrated distributions to files
*....int_sb and int_b
*
      open(31,name='int_sb',status='unknown')
      open(32,name='int_b',status='unknown')
      do i=1,m
         write(32,*)integr_b(i)
      enddo
      do i=1,m_sb
         write(31,*)integr_sb(i)
      enddo
```

```
      close(31)
      close(32)

*
*....Calculating the confidence for bg. only
*
      cl_b=0.
      i=1
      DO WHILE(expt.GE.result_b(1,i))
         cl_b=integr_b(i)
         i=i+1
      ENDDO


*
*....And signal+background....
*
      cl_sb=0.
      i=1
      DO WHILE(expt.GE.result_sb(1,i))
         cl_sb=integr_sb(i)
         i=i+1
      ENDDO
*
*....Computing derived quantities....
*

*....the observed signal confidence
      cl_s=cl_sb/cl_b
      gen_xisq=(2*stot)-wt_expt

*
*....Preparing calculations of expected CL_s and CL_sb
*
      DO i=1,no_bins
         interm_s(i)=integr_sb(i)/integr_b(i)
         interm_sb(i)=result_b(2,i)*integr_sb(i)
      ENDDO

      DO i=1,no_bins
         interm_s(i)=result_b(2,i)*interm_s(i)
      ENDDO

      DO i=2,no_bins
```

```
         interm_s(i)=interm_s(i)+interm_s(i-1)
         interm_sb(i)=interm_sb(i)+interm_sb(i-1)
      ENDDO

*
*....<CL_s> and <CL_sb>!
*
      cl_s_infty=interm_s(no_bins)  !the expected signal
      cl_sb_infty=interm_sb(no_bins)


      PRINT 799
 799  FORMAT (/3x,'CL_sb              CL_b            CL_s
     & <CL_s>           <CL_sb>          <CL_b>')
      PRINT 899,cl_sb,cl_b,cl_s,acls,aclsb,aclb
 899  FORMAT(E16.8,1X,E16.8,1X,E16.8,1X,E16.8,1X,E16.8,1X,E16.8)
      PRINT *,'   '


      END
```

Appendix B

```
      program susypar
*
*....Program that computes the excluded M_2/mu plane in MSSM
*
      implicit none

      double precision m2,mw,mz,m1,m0,k1,k2,beta,theta,pi
      double precision u(2,2),v(2,2)
      double precision sigma(2,2),detX,Ql,Qr
      double precision Gf,g1,g2,lambda,gamma,branching_ratio
      double precision m,m_prim,mu,w_width,m_rot

*
*....This is the varibles concerning the diagonalization of the
*....neutralino mixing matrix. Borrwed from SUSYGEN2.2,
*....see IC/HEP/97-5.
*
      real fma(4,4),wr(4),dr(4,4),work(16),vtemp(4)
      double precision neut_mass(4),neut_phase(4)
      double precision vo(4,4),neut_mix(4,4),neut_dmatrix(4,4),a1,a2
      double precision temp,temp1,t1,t2,t3,t4
      integer ierr

      double precision w,w_root,bv

*
*....Counting variables
*

      integer i,j

*
*....variables concerning HBOOK
```

```
*
      logical hexist
      external hexist

      integer mwp,h
      parameter(mwp=11200000)
      common/pawc/h(mwp)
      call hlimit(11200000)


*
*....Reading the value of tan(beta) from file betavalue
*
      open(10,name='betavalue',status='old')
      read(10,*)bv
      close(10)

*
*....Reading the value of the branching ratio of
*....W^+ -> X_0^+ X_0^0 from file br_rate
*
      open(11,name='br_rate',status='old')
      read(11,*)branching_ratio
      close(11)

*
*....Values of constants
*

      pi=3.1415927
      mw=80.41               !W-boson mass
      mz=91.187              !Z-boson mass
      beta=atan(bv)          !mixing angle between Higgses vac. exp. value
      theta=asin(sqrt(0.23124)) !Weak mixing angle
      Gf=1.16639e-5          !Fermi coupling constant
      w_width=2.06*branching_ratio !2.06 GeV is the (W -> anything) width

*
*....Pauli matrix #3
*

      sigma(1,1)=1
      sigma(1,2)=0
```

```
      sigma(2,1)=0
      sigma(2,2)=-1

*
*....HBOOK histogram booking
*

      CALL hbook2(123,'M_2/mu plane',801,-200.,200.,401,0.,200.,0.)

*
*....Neutralino Mixing Matrix N(ij)
*

      vo(1,1)=cos(theta)
      vo(1,2)=-sin(theta)
      vo(1,3)=0.
      vo(1,4)=0.

      vo(2,1)=sin(theta)
      vo(2,2)=cos(theta)
      vo(2,3)=0.
      vo(2,4)=0.

      vo(3,1)=0.
      vo(3,2)=0.
      vo(3,3)=cos(beta)
      vo(3,4)=sin(beta)

      vo(4,1)=0.
      vo(4,2)=0.
      vo(4,3)=-sin(beta)
      vo(4,4)=cos(beta)


*
*....Varying some of the parameters in the MSSM theory: M_2 & mu
*

      DO mu=-200.,200.,0.5

         DO m=0.,200.,0.5

*
*....The neutralino mixing matrix (this is copied from SUSYGEN):
```

```
*
            m_prim=m*5./3.*sin(theta)**2/cos(theta)**2

*
*....This is the neutralino mixing matrix
*
            fma(1,1)=m_prim*cos(theta)**2+m*sin(theta)**2
            fma(2,1)=(m-m_prim)*sin(theta)*cos(theta)
            fma(3,1)=0.
            fma(4,1)=0.
            fma(1,2)=(m-m_prim)*sin(theta)*cos(theta)
            fma(2,2)=m_prim*sin(theta)**2+m*cos(theta)**2
            fma(3,2)=mw/cos(theta)
            fma(4,2)=0.
            fma(1,3)=0.
            fma(2,3)=mw/cos(theta)
            fma(3,3)=mu*(2.*sin(beta)*cos(beta))
            fma(4,3)=-mu*(cos(beta)**2-sin(beta)**2)
            fma(1,4)=0.
            fma(2,4)=0.
            fma(3,4)=-mu*(cos(beta)**2-sin(beta)**2)
            fma(4,4)=-mu*(2.*sin(beta)*cos(beta))

*
*....Diagonalizing the mixing matrix in order to find
*....the neutralino mass egienstates
*
            call eisrs1(4,4,fma,wr,dr,ierr,work)
            if(ierr.ne.0)then
               print *,'FUBAR!!!!!'
               stop
            endif

            do i=1,4
               neut_mass(i)=dble(abs(wr(i)))
               neut_phase(i)=dble(sign(1.,wr(i)))
            enddo

            do i=1,4
               do j=i+1,4
                  if(neut_mass(i).gt.neut_mass(j))then
                     call ucopy(dr(1,j),vtemp,4)
                     temp=abs(neut_mass(j))
```

```
                  temp1=neut_phase(j)
                  call ucopy(dr(1,i),dr(1,j),4)
                  neut_mass(j)=neut_mass(i)
                  neut_phase(j)=neut_phase(i)
                  call ucopy(vtemp,dr(1,i),4)
                  neut_mass(i)=temp
                  neut_phase(i)=temp1
               endif
            enddo
         enddo

         do i=1,4
            do j=1,4
               neut_dmatrix(i,j)=dble(dr(i,j))
            enddo
         enddo

         do i=1,4
            do j=1,4
               neut_mix(i,j)=vo(j,1)*neut_dmatrix(1,i)+vo(j,2)*
     &neut_dmatrix(2,i)+vo(j,3)*neut_dmatrix(3,i)+vo(j,4)*
     &neut_dmatrix(4,i)
            enddo
         enddo
*
*....End of SUSYGEN's matrix-diagonalizing part
*

*
*....These are the chargino mixing matrices
*....(since the chargino mixing matrix is a 2x2 matrix,
*....dagonalization has been done analytcal):
*
         if(tan(beta).gt.1.)then
            t1=1.
            if((m*cos(beta)+mu*sin(beta)).gt.0.)then
               t2=1.
            else
               t2=-1.
            endif
            if((m*sin(beta)+mu*cos(beta)).gt.0)then
               t3=1.
            else
               t3=-1.
```

```
               endif
               t4=1.
            elseif(tan(beta).lt.1.)then
               if((m*cos(beta)+mu*sin(beta)).gt.0.)then
                  t1=1.
               else
                  t1=-1.
               endif
               t2=1.
               t3=1.
               if((m*sin(beta)+mu*cos(beta)).gt.0)then
                  t4=1.
               else
                  t4=-1.
               endif
            endif

*
*....This is part of the chargino mixing matrix
*
            w=(m**2+mu**2+2*mw**2)**2-4*(m*mu-mw**2*sin(2*beta)**2)

*
*....Since w enters the matrix under a sqare root, negative values aren't
*....allowed!
*

            if(w.lt.0.)then
               w=0.
               print *,'Just adjusted for negative roots!'
            endif



*
*....The different matrix elements of the chargino mixing matrix.
*....These expressions are found analytical.
*
            u(1,2)=t1/sqrt(2.)*sqrt(1+(m**2-mu**2-2*mw**2*cos(2*beta))/
     &sqrt(w))

            u(2,1)=t1/sqrt(2.)*sqrt(1+(m**2-mu**2-2*mw**2*cos(2*beta))/
     &sqrt(w))

            u(2,2)=t2/sqrt(2.)*sqrt(1-(m**2-mu**2-2*mw**2*cos(2*beta))/
```

```
     &sqrt(w))

            u(1,1)=-t2/sqrt(2.)*sqrt(1-(m**2-mu**2-2*mw**2*cos(2*beta))
     &/sqrt(w))

            v(2,1)=t3/sqrt(2.)*sqrt(1+(m**2-mu**2+2*mw**2*cos(2*beta))/
     &sqrt(w))

            v(1,2)=-t3/sqrt(2.)*sqrt(1+(m**2-mu**2+2*mw**2*cos(2*beta))
     &/sqrt(w))

            v(2,2)=t4/sqrt(2.)*sqrt(1-(m**2-mu**2+2*mw**2*cos(2*beta))
     &/sqrt(w))

            v(1,1)=t4/sqrt(2.)*sqrt(1-(m**2-mu**2+2*mw**2*cos(2*beta))
     &/sqrt(w))


*
*....The coupling of the chargino and the neutralino to the W:
*

            Ql=(neut_mix(1,2)*v(1,1))-
     &(1./sqrt(2.)*neut_mix(1,4)*v(1,2))

            Qr=(neut_mix(1,2)*u(1,1))+
     &(1./sqrt(2.)*neut_mix(1,3)*u(1,2))

*
*....Calculating the chargino mass
*

            m_rot=0.5*(m**2+mu**2+2*mw**2-sqrt((m**2-mu**2)**2+
     &             4*mw**4*(cos(2*beta))**2+
     &             4*mw**2*(m**2+mu**2+2*m*mu*sin(2*beta))))


            m2=sqrt(m_rot)  !the  chargino mass
            m1=neut_mass(1) !the  neutralino mass

*
*....The ratio between the chargino/neutralino masses and the W mass
*
            k1=m2/mw
```

```
            k2=m1/mw

*
*....a few of the constants in the Kalinowsky-Zerwas equation
*

            lambda=(1-(k1**2)-(k2**2))**2-
     &(4*(k1**2)*(k2**2))
            g1=((Gf)*(mw**3)*sqrt(lambda))/(6*sqrt(2.)*pi)
            g2=(2-(k1**2)-(k2**2)-((k1**2)-(k2**2))**2)

*....This is the Kalinowski-Zerwas equation as found in Phys. Rep. 117 (1985):

            gamma=g1*(g2*((Ql**2)+(Qr**2))+(12*k1*k2*Ql*Qr))

*
*....Idiotic result-preventing check
*

            if(m1+m2.lt.0.)then
               print *,m1,m2,m1+m2
               print *,'?'
            endif

*
*....Histogramming the physical possible results:
*

            if((m1+m2).le.mw)then !To check if m1+m2 mass less than W-mass.
                                  !if not -> unphysical reaction!

*
*....Checking whether or not the W width computed in the Haber-Kane
*....equation is less or greater than the experimental W width.
*....These are all for the SUSY decay, with sneutrino og neutralino
*....nearly mass degenerate:
*

*
*....Excluded results are histogrammed
*
               if(gamma.gt.w_width)then
                  call hfill(123,real(mu),real(m),real(gamma))
               endif
```

```
            endif
999         continue
         ENDDO
      ENDDO
      call hrput(0,'susy.hst','n')
      END
```

Bibliography

[1] Donoghue, Golowich, Holstein, *Dynamics of the Standard Model*, Cambridge University Press 1992, ISBN 0 521 36288 1 hardback.

[2] Gunion, Haber, Kane, Dawson, *The Higgs Hunter's Guide*, Addison-Wesley Publishing Company, ISBN 0-201-50935-0.

[3] Halzen, Martin, *Quarks & leptons, An introductory course in Modern Particle Physics*, John Wiley & Sons, ISBN 0-471-88741-2 hardback.

[4] Katsanevas, Morawitz, *SUSYGEN 2.2 - A Monte Carlo Event generator for MSSM Sparticle Production at e^+e^- colliders*, IC/HEP/97-5.

[5] C.Caso, *et al.*(Particle Data Group), European Physical Journal **C3**, 1(1998).

[6] H.E.Haber, G.L.Kane, *The search for supersymmetry: Probing physics outside the standard model*, Phys. Rep. 117 (1985).

[7] J.Kalinowsky, P.M.Zerwas, *Decays of W bosons to charginos and neutralinos*, Phys. Lett. B 400 (1997) 112.

[8] C.Caso *et* al. (Particle Data Group), European Physical Journal **C3**, 1 (1998).

[9] A.Perrotta, T.Rovelli, N.Tinti, *Search for SUSY decays of the W*, DELPHI Note 98-166 PHYS 806, 10 November, 1998.

[10] Crzystof Cieslik, *The DELPHI detector at CERN's LEP collider*, http://home.cern.ch/ offline/physics/delphi-detector.html [online]. Accesed 26 May, 1999.

[11] DELPHI collaboration, *The DELPHI detector* Nuclear Instruments & Methods **A303**(1991) 233.

[12] A. L. Read *Optimal Statistical Analysis of Search Results based on the Likelihood Ratio and its Application to the Search for the MSM Higgs Boson at $\sqrt{s} = 161$ and 172 GeV*, DELPHI Note 97-158 PHYS 737, 29 October, 1997.

[13] Glen Cowan *Statistical data analysis*, Oxford University press, 1998, ISBN 0 19 850155 2 Paperback.

[14] S. L. Meyr *Data analysis for scientists and engineers*, John Wiley & sons, 1975, ISBN 0-471-59995-6.

[15] Thomas Junk *Confidence Level Computation for Combining Searches using the Likelihood Ratio*, OPAL Technical note TN-570, 7 October, 1998.

[16] F. DiLodovico *Report from the LEP Higgs workinggroup* http://www.cern.ch/LEPHIGGS/talks/LEPC-sept98.ps [online] Accesed 21 june, 1999.

[17] P. Abreu et al., DELPHI Collaboration, *Search for neutral Higgs boson in e^+e^- collitions at $\sqrt{s}$=183 GeV*, CERN-EP 99-06.

[18] G. Altarelli, T. Sjöstrand, F. Zwirner (editors), *CERN Report* CERN 96-10 (1996), 1999.

[19] G. Borisov Combined b-tagging, Nuclear Instruments & Methods **A417** (1998) 384.

[20] Robert D.Cousins, Virgil L.Highland *Incorporating systematic uncertainties into an upper limit*, Nuclear Instruments & Methods **A320**(1992) 331.

[21] Thomas Junk *FORTRAN code* http://home.cern.ch/ thomasj/searchlimits/eclsyst.f [online] Accesed 23 july, 1999.